

Connect Control Theory with the Practical World

Replication of power grid dynamic events & control design for inverter-based resources

MIT Energy & Infrastructure Systems: Modeling, Computing, and Control (EIMC2) Seminar Series

May 1st, 2025

Presenter: Lingling Fan, Professor, FIEEE

Collaborator: Zhixin Miao, Professor

Smart Grid Power Systems Lab

University of South Florida

<http://power.eng.usf.edu>





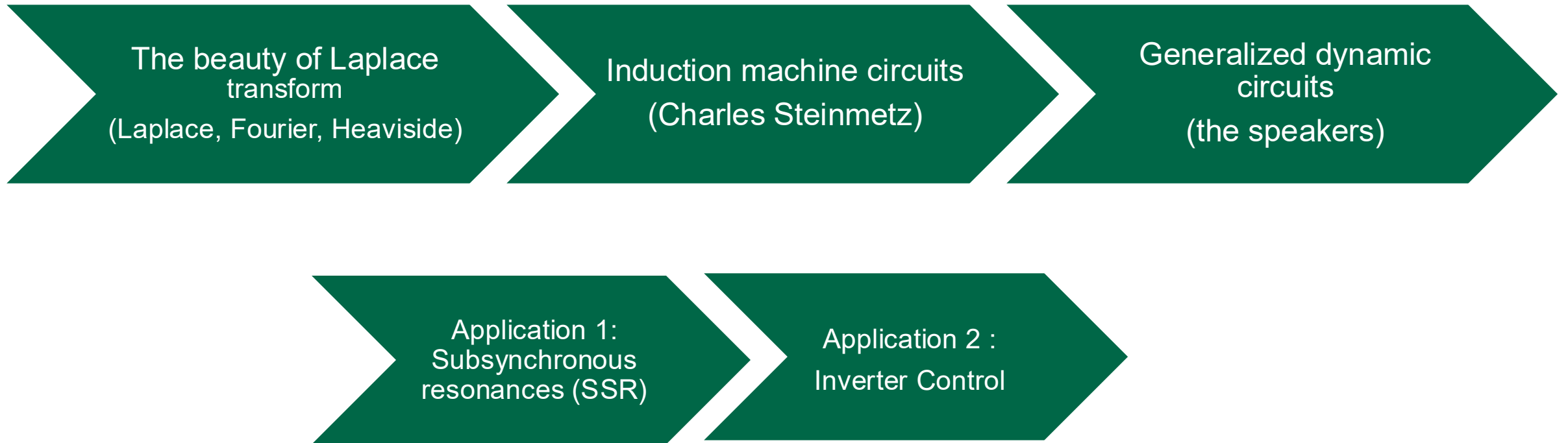
U.S. DEPARTMENT
of **ENERGY**

DE-EE0011474

SPRING: Stability Prediction for IBR-Penetrated Grids Enabled by Digital Twins



Outline



From Laplace transform to Heaviside's operational calculus

It took a century for a math concept to become a practical tool in circuit analysis

Laplace transform: 1814



Pierre-Simon Laplace (1749-1827)



Joseph Fourier (1768-1830)



Oliver Heaviside (1850-1925)

$$F(s) = \int_0^{\infty} f(t)e^{-st} dt, \text{ (Eq. 1)}$$



If $f(t)$ is in the form of Ke^{st}

$$f(t) = F(s) e^{st}$$



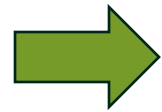
$$f(t) = F(j\omega) e^{j\omega t}$$

Oliver Heaviside's operational calculus (1893):

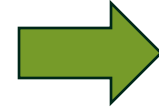
$$v = iR$$

$$i = Cpv \text{ from } v = \frac{1}{c} \int i dt$$

$$v = Lpi \text{ from } v = L \frac{di}{dt}$$



$$Ri + L \frac{di}{dt} = v$$



$$(R + Lp)i = v$$

$$i = \frac{v}{Z} = \frac{1}{(R + Lp)} \mathbf{1} = \frac{1}{R} \times \frac{R}{Lp} \frac{1}{\left(1 + \frac{R}{Lp}\right)} \mathbf{1} = \frac{1}{R} \times \frac{1}{\tau p} \frac{1}{\left(1 + \frac{1}{\tau p}\right)} \mathbf{1},$$

$$\left(1 + \frac{1}{\tau p}\right)^{-1} = 1 - \frac{1}{\tau p} + \left(\frac{1}{\tau p}\right)^2 - \left(\frac{1}{\tau p}\right)^3 + \dots$$

$$\frac{\mathbf{1}}{p^n} \mathbf{1} = \frac{t^n}{n!}$$

Treat d/dt as an operator p ,
 $1/p$ is integration.

$$p \longleftrightarrow s$$

Taylor's expansion

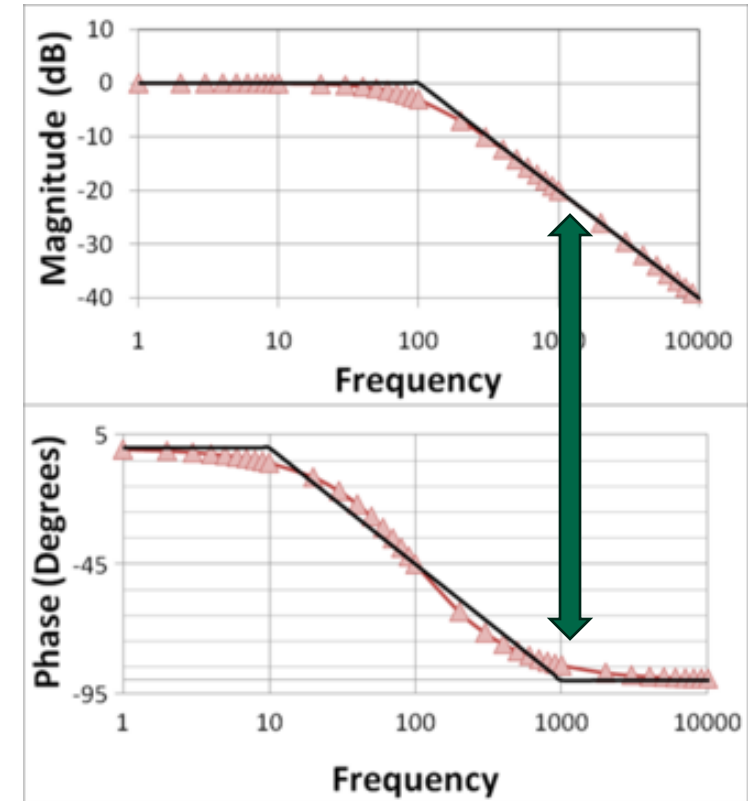
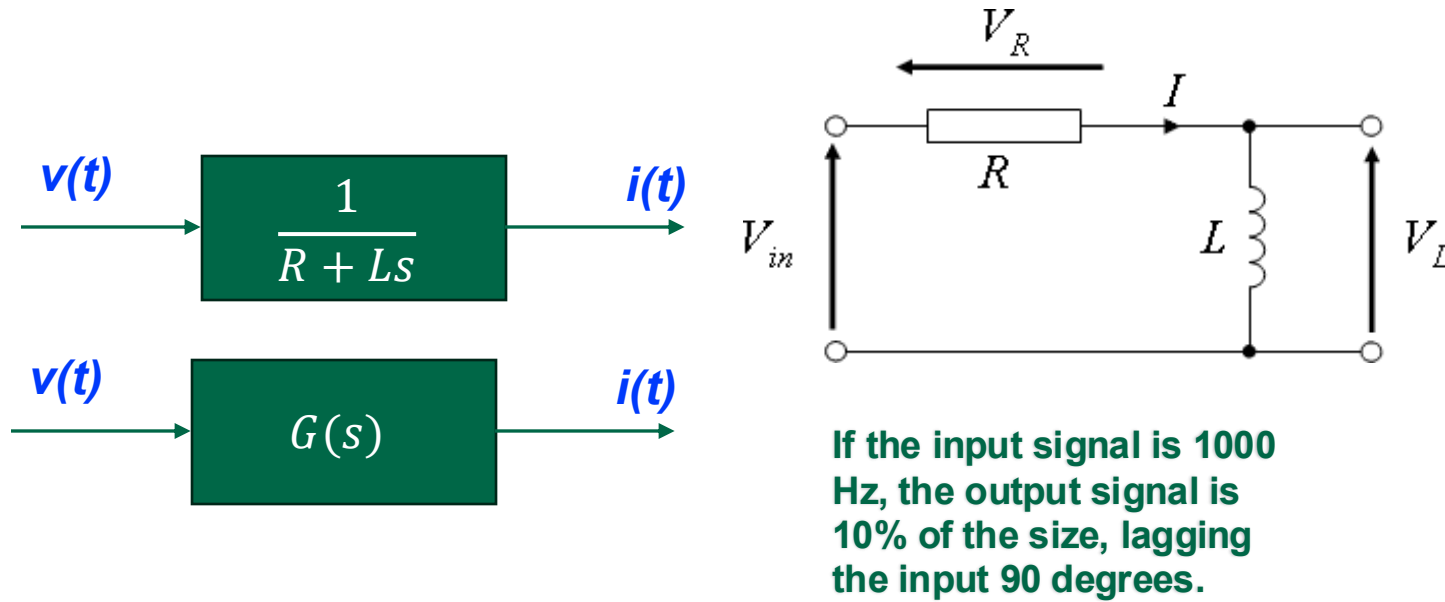
$$i = \frac{1}{R} \times \frac{1}{\tau p} \left[1 - \frac{1}{\tau p} + \left(\frac{1}{\tau p}\right)^2 - \left(\frac{1}{\tau p}\right)^3 + \dots \right] \mathbf{1}$$

$$i = \frac{1}{R} \times \left[\frac{t}{\tau} - \frac{1}{2!} \left(\frac{t}{\tau}\right)^2 + \frac{1}{3!} \left(\frac{t}{\tau}\right)^3 - \dots \right]$$

$$i = \frac{1}{R} \left[1 - e\left(-\frac{t}{\tau}\right) \right]$$

EE fundamentals: signals & systems

https://en.wikipedia.org/wiki/Bode_plot



If the input is $e^{j\omega t}$, the **steady-state** output is $G(j\omega)e^{j\omega t}$

If the input signal is e^{st} , the **steady-state** output is $G(s)e^{st}$

If $v(t) = 1(t) = e^{0t}$, the **steady-state** $i(t)$ is $\frac{1}{R}1(t)$.

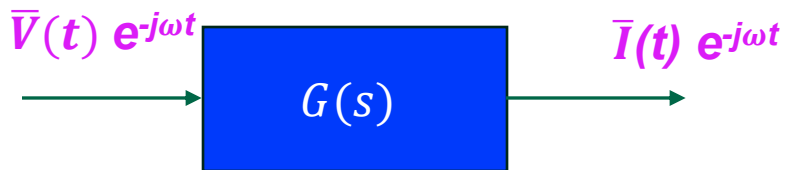
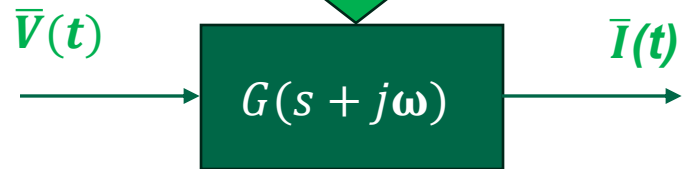
If $v(t) = e^{st}$, the **steady-state** $i(t)$ is $\frac{1}{R+Ls}e^{st}$.

More: frame conversion



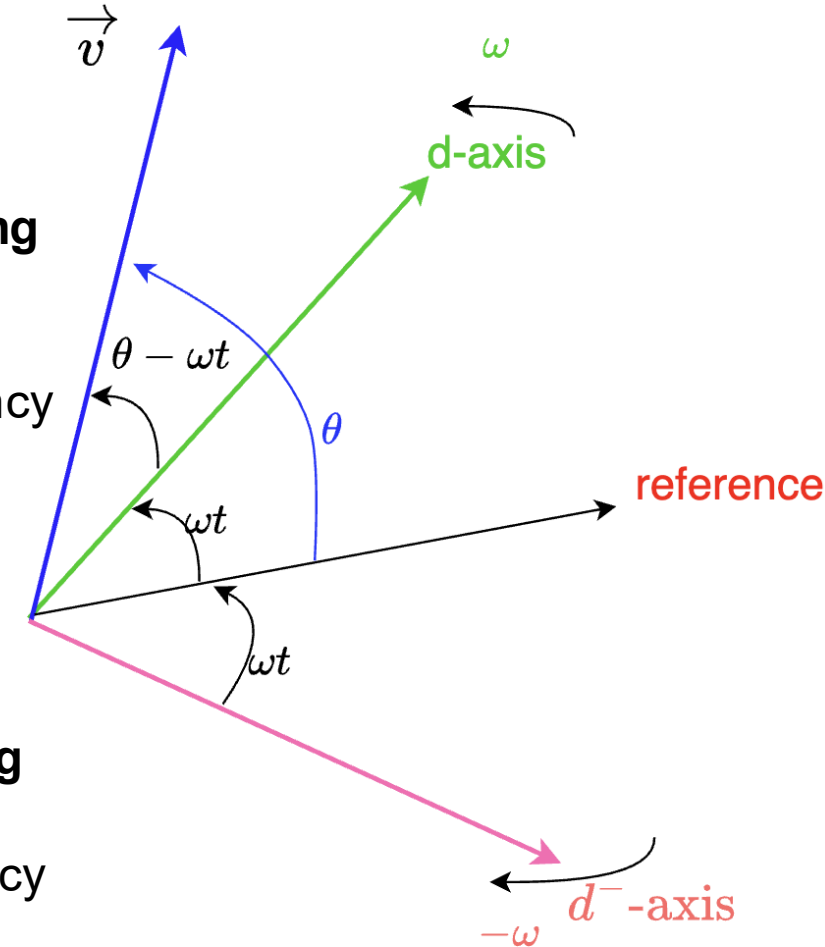
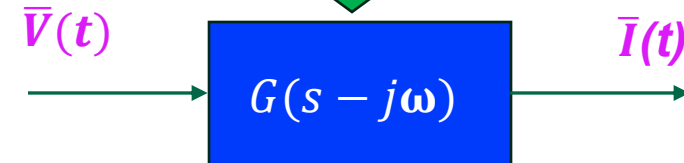
If the input signal is $e^{st} e^{j\omega t}$, the output signal is $G(s+j\omega)e^{st} e^{j\omega t}$

- The signals are **viewed in a rotating frame with a speed of ω** ;
- The signals' phasors at this frequency ω are examined.



If the input signal is $e^{st} e^{-j\omega t}$, the output signal is $G(s-j\omega)e^{st} e^{-j\omega t}$

- The signals are viewed **in a rotating frame with a speed of $-\omega$** ;
- The signals' phasors at this frequency $-\omega$ are examined.

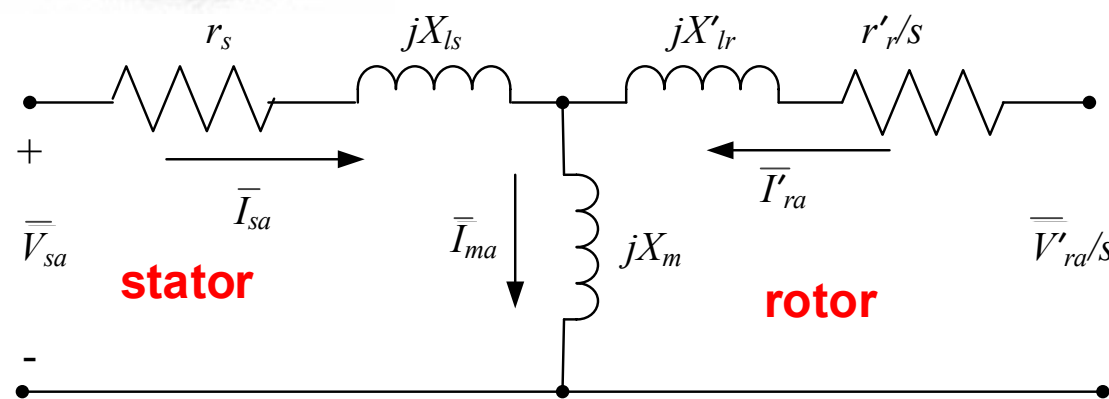


Circuits of a 3-phase AC machine: from Steinmetz to the speakers (a century apart!)



Charles P. Steimetz' phasor-impedance model of IM

Steady-state phasor-impedance representation



Critical relationship: Faraday's Law

$$e_{sa} = \frac{d\lambda_{sa}}{dt} = \omega_e L_m \hat{i}_m \cos \left(\omega_e t + \theta_{m0} + \frac{\pi}{2} \right)$$

$$e_{ra} = \frac{d\lambda_{ra}}{dt} = \frac{N_r}{N_s} s \omega_e L_m \hat{i}_m \cos \left(s \omega_e t + \theta_{m0} + \frac{\pi}{2} \right).$$

Significance:

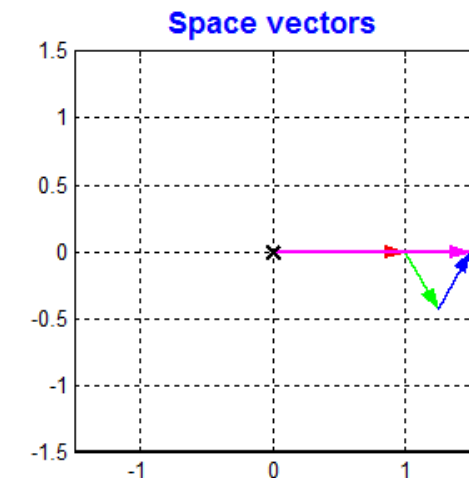
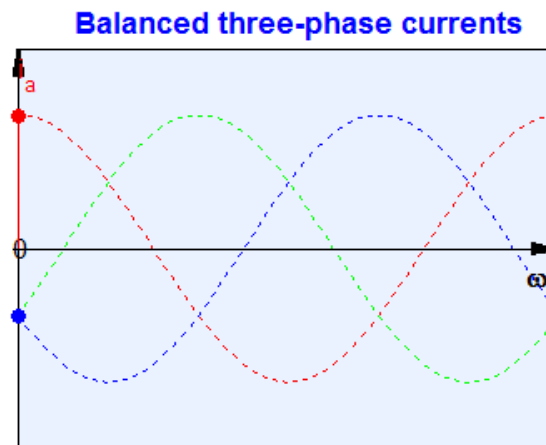
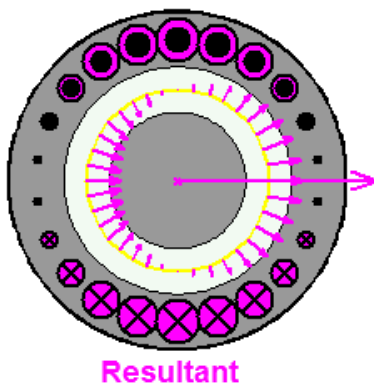
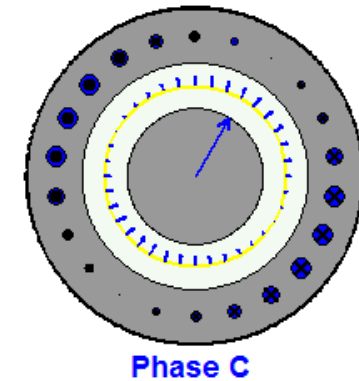
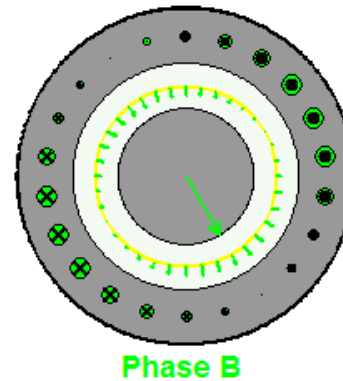
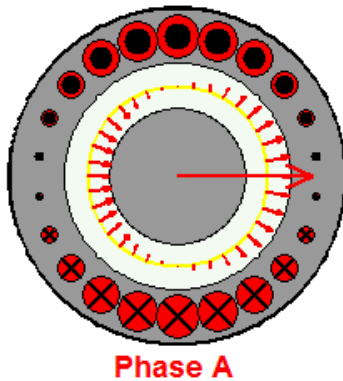
- The **stator circuit** (frequency 60Hz) and the **rotor circuit** (at slip frequency, eg., 10 Hz) are connected through a **rotating magnetic** field set up by both stator & rotor currents. A motor is rotating at 50 Hz.
- **Time-domain to frequency domain conversion**
 - Phasors of **different frequencies**, instead of instantaneous variables are used.
- **Mechanical motion is included by the slip: 1-rotating speed/stator frequency (10/60 or 1-50/60).**

Steinmetz translated physics to math/circuit expressions

- **Step 1:** Three-phase stator currents form a rotating magnetic field.
- **Step 2:** Faraday's Law & induction
 - The rotor circuit has induced current. This current sets up a rotating magnetic field.
- **Step 3:** Motion. Two fields interact and generate a torque. The rotor rotates.
- **Step 4:** Achieve steady state.
 - The rotor is rotating at a speed of ω_m , while the rotor circuit flows ac electricity of slip frequency. The stator circuit flows ac electricity of a nominal frequency.

Forming a rotating magnetic field

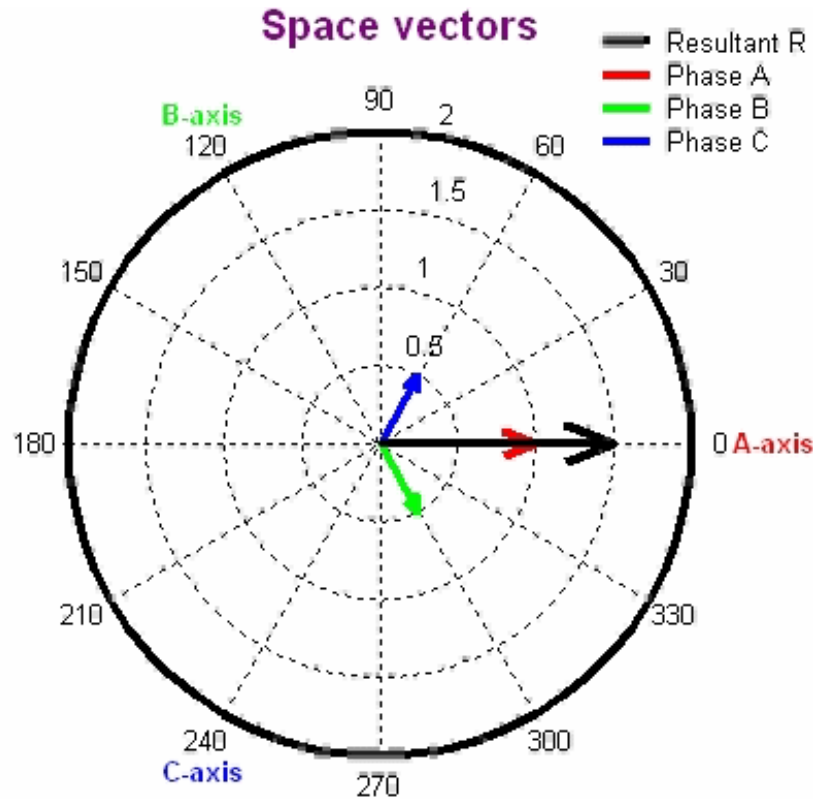
<https://www.ece.umn.edu/users/riaz/animations/abcvec.html> (animation credit to Riaz)



Forming a rotating magnetic field



Edith Clarke



Clarke' transform:

$$\vec{v} = \frac{2}{3} \left(v_a + e^{j\frac{2\pi}{3}} v_b + e^{-j\frac{2\pi}{3}} v_c \right)$$



$$\begin{aligned} \vec{v} &= \frac{2}{3} \hat{v} \left(\cos(\theta) + e^{j\frac{2\pi}{3}} \cos\left(\theta - \frac{2\pi}{3}\right) + e^{-j\frac{2\pi}{3}} \cos\left(\theta + \frac{2\pi}{3}\right) \right) \\ &= \frac{1}{3} \hat{v} \left(e^{j\theta} + \cancel{e^{-j\theta}} + e^{j(\frac{2\pi}{3} + \theta - \frac{2\pi}{3})} + \cancel{e^{j(\frac{2\pi}{3} - \theta + \frac{2\pi}{3})}} + e^{j(-\frac{2\pi}{3} + \theta + \frac{2\pi}{3})} + \cancel{e^{j(-\frac{2\pi}{3} - \theta + \frac{2\pi}{3})}} \right) \\ &= \hat{v} e^{j\theta}. \end{aligned}$$

The time-domain signals: B lags A, C lags B

Faraday's Law

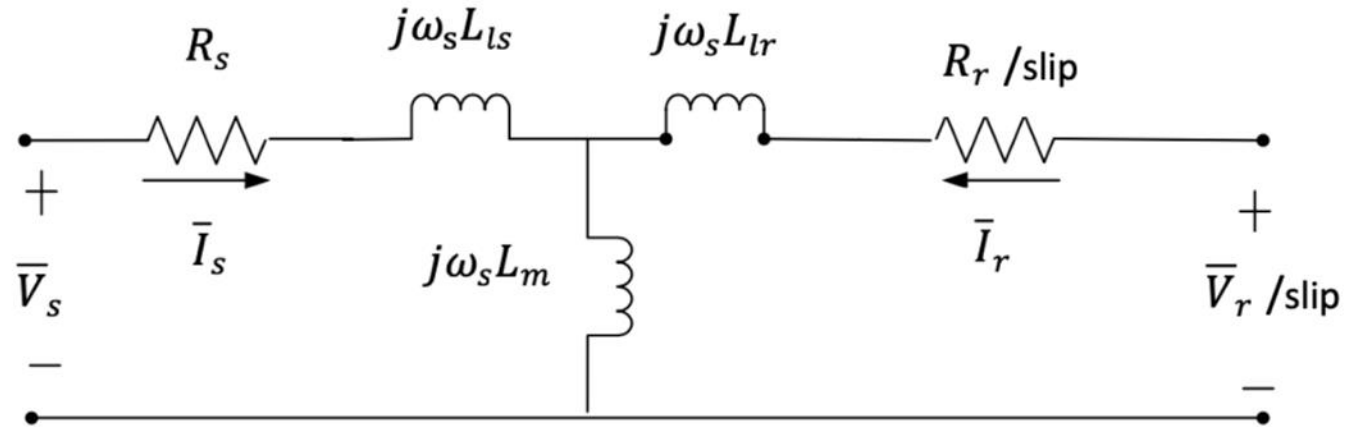
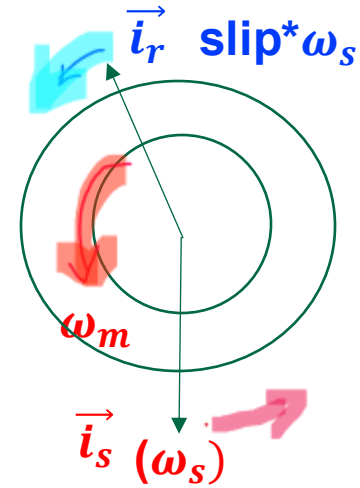
$$\vec{\psi}_m = L_m(\vec{i}_s + \vec{i}_r e^{j\omega_m t}) = L_m(\bar{I}_s + \bar{I}_r) e^{j\omega_s t}, \text{ viewed from the stator frame,}$$

$$\vec{\psi}_m^r = L_m(\vec{i}_s e^{-j\omega_m t} + \vec{i}_r) = L_m(\bar{I}_s + \bar{I}_r) e^{j\text{slip} \times \omega_s t}, \text{ viewed from the rotor frame.}$$

$$\vec{e}_s = \underbrace{j\omega_s L_m(\bar{I}_s + \bar{I}_r)}_{\bar{E}_s} e^{j\omega_s t},$$

$$\vec{e}_r = \underbrace{j\text{slip} \times \omega_s L_m(\bar{I}_s + \bar{I}_r)}_{\bar{E}_r} e^{j\text{slip} \times \omega_s t}.$$

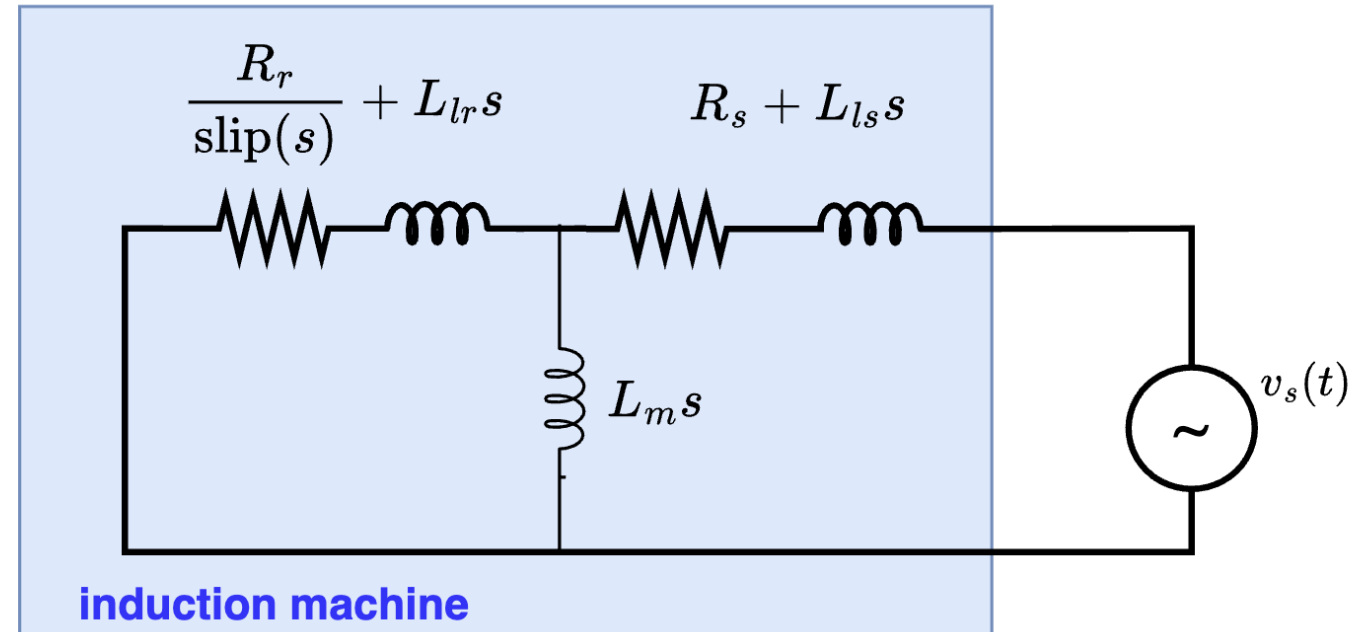
$$\bar{E}_r = \text{slip} \times \bar{E}_s, \implies \bar{E}_s = \frac{\bar{E}_r}{\text{slip}} = \omega_s L_m (\bar{I}_s + \bar{I}_r).$$



The rotor circuit's frequency is the slip frequency. To ensure the two circuits in their respective phasor domain can be interconnected, the rotor circuit's voltage and impedance is scaled: divided by the slip.

From the steady-state circuit to a general dynamic circuit

- Assumption of the steady-state circuit is that the input signals (stator voltage) are in the format of $e^{j\omega_{st}}$.
- Impedances are evaluated for
 - $s = j\omega_s$
- Therefore, we may lift the steady-state circuit to a dynamic circuit by replacing $j\omega_s$ using s

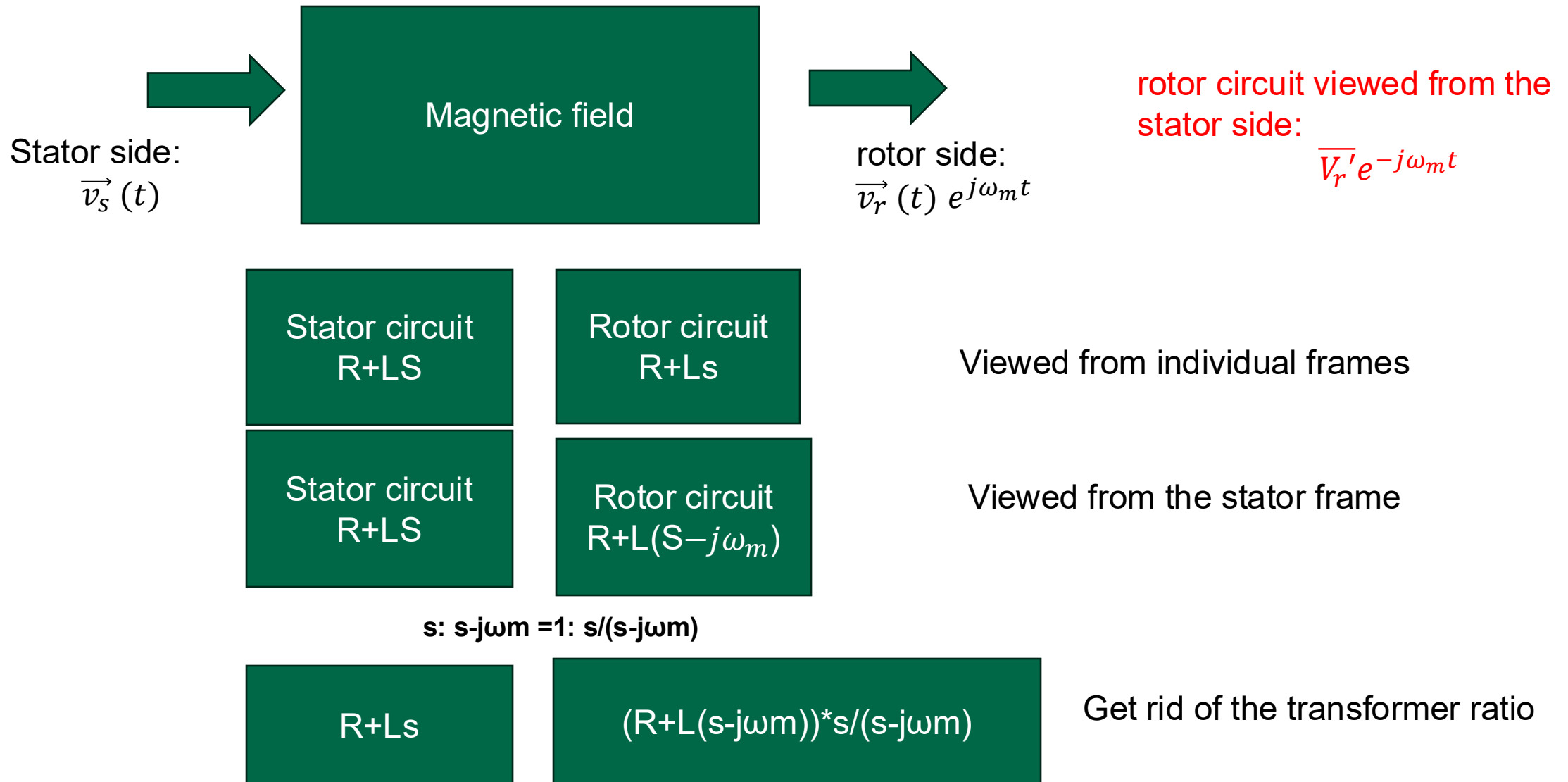


$$\text{slip} = 1 - \frac{\omega_m}{\omega_s} = 1 - \frac{j\omega_m}{j\omega_s} = 1 - \frac{j\omega_m}{s}$$

If the excitation frequency $\omega < \omega_m$ the rotating speed, slip < 0 . The system has a **negative resistance** at that frequency.

- Fan, L. and Miao, Z., 2012. Nyquist-stability-criterion-based SSR explanation for type-3 wind generators. *IEEE Transactions on Energy Conversion*, 27(3), pp.807-809.
- Fan, L. and Miao, Z., 2023. *Modeling and stability analysis of inverter-based resources*. CRC Press.

Based on signals and systems:



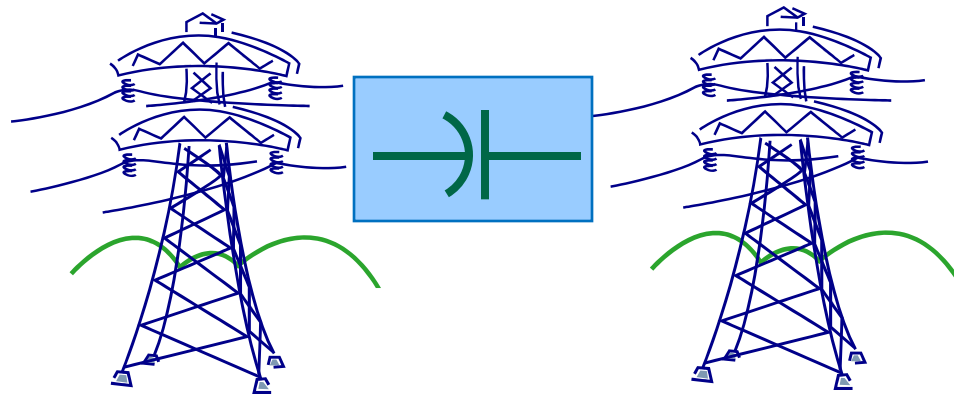
Application 1: Why do SSRs happen in series compensated networks?

Subsynchronous resonances (SSR)

- **Series compensation + AC machines (induction motors, synchronous generators, type-3 wind turbines)**
 - 1930s: The first series capacitor application to transmission network. In 1937, Charles Concordia **predicted** the potential for adverse interactions between the series capacitor and turbine generators.
 - 1940s: series capacitor-induced oscillations (12 Hz) in a distribution system supplying power to a large induction motor in a mine in the west coast.
 - 1930s-1970s: self-excited oscillations in long distance transmission with series caps.
 - In the 1970s, Mohave synchronous generator unit rotor damage.
 - “Investigations determined that an electrical resonance at 30.5 Hz produced torque at 29.5 Hz (the 60 Hz complement frequency), which was near coincident with the frequency of the second torsional vibration-mode of the turbine-generator at 30.1 Hz. ”
 - 2009, 2017, 2023: South Texas type-3 wind farm SSR events.

Subsynchronous resonance (SSR) due to LC resonance

- It happened before in 1970s at Nevada's Mohave power plant.
- One of the power plant (1,580 MW)'s synchronous generator experienced growing vibration in its shaft, causing damage →
- Reason: 30.1 Hz oscillations in the mechanical side triggered by LC resonance from the electrical side.
- If the **electric LC frequency + shaft mode frequency = 60 Hz**, **torsional interaction may occur**.



Series capacitors can introduce LC resonances.

Source: Jonathan Rose, ERCOT and the following two references

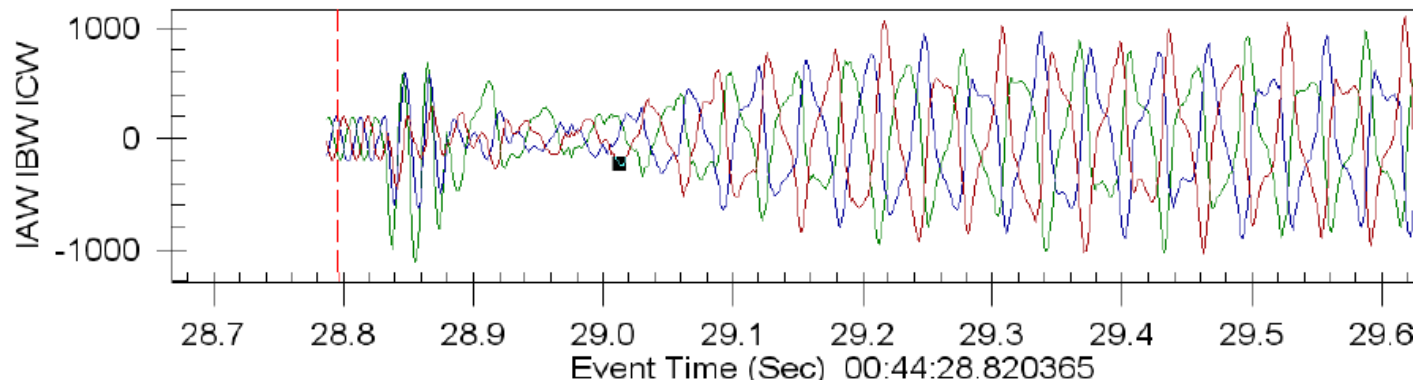
D. Baker, G. Boukarim, "Subsynchronous Resonance Studies and Mitigation Methods for Series Capacitor Applications," IEEE 2005.

D. Walker, D. Hodges, "Results of Subsynchronous Resonance Test At Mohave," IEEE 1975.

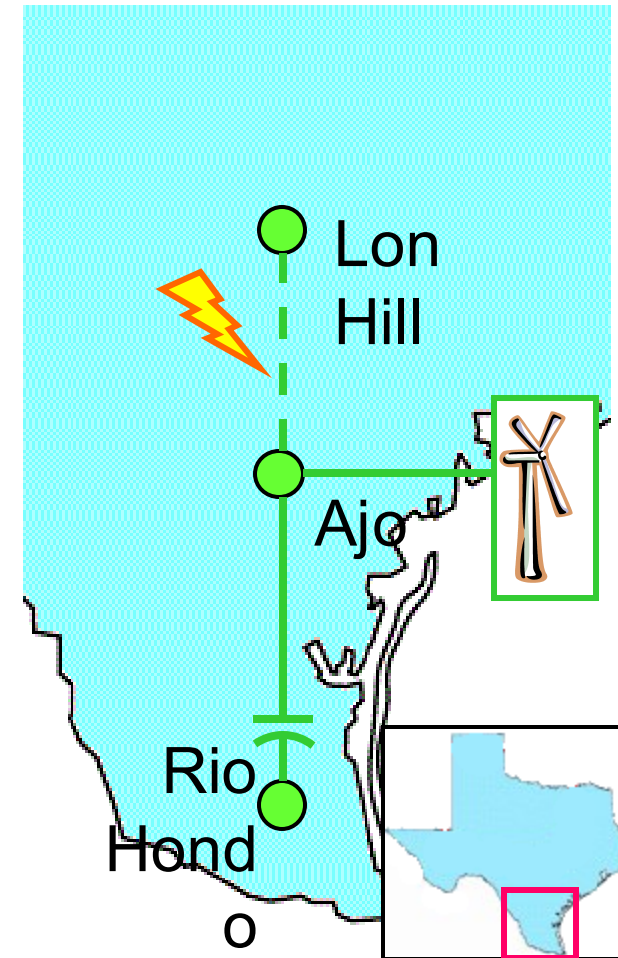
Solution: Filters added in transformers' grounding circuit to block the LC modes entering the generator; Generators have SSR protection installed.

South Texas 2009 Event

- Series capacitors installed on Lon Hill – Rio Hondo 345 kV long line in South Texas.
- A cluster of wind farms (DFIG) connected to Ajo.
- A fault caused LonHill – Ajo line to trip, leaving wind farms radially connected to series caps.
- Very **high currents** resulted in damage.

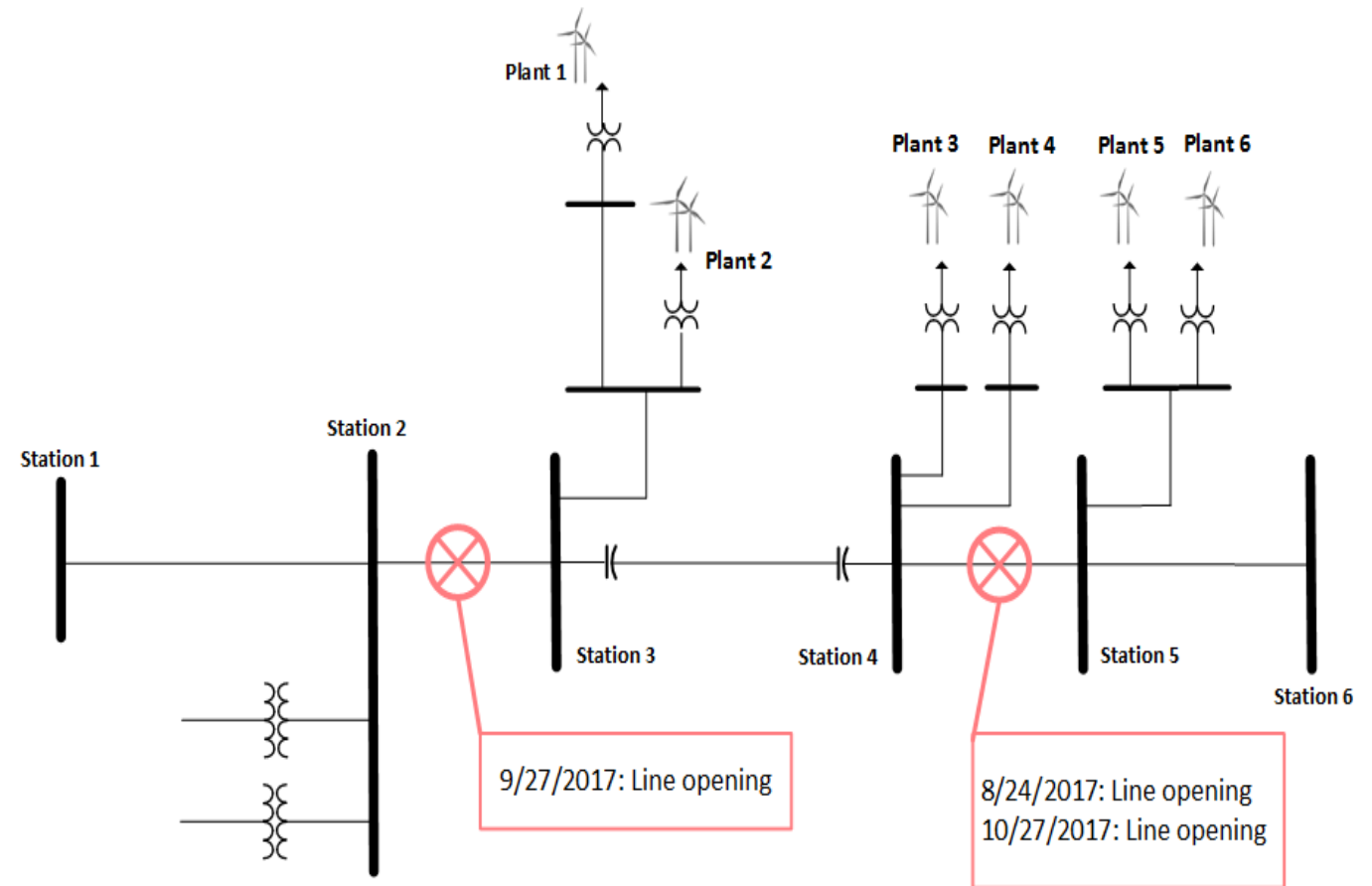


Reference: Chapter 2.2, Task Force Report from IEEE PES Task Force Modeling Subsynchronous Oscillations in Wind Energy Interconnected Systems (Wind SSO TF), by Yunzhi Cheng, Jonathan Rose, John Schmall and Fred Huang



South Texas 2017 Events

- Three type-3 wind SSR events occurred in South Texas in 2017
- Wind plants (DFIG) tripped by SSR protection
- Challenges: The original SSR study failed to capture the SSR risk



Reference: Chapter 2.2, Task Force Report from IEEE TR-80 : Modeling Subsynchronous Oscillations in Wind Energy Interconnected Systems (Wind SSO TF), by Yunzhi Cheng, Jonathan Rose, John Schmall and Fred Huang

South Texas 2017 Events

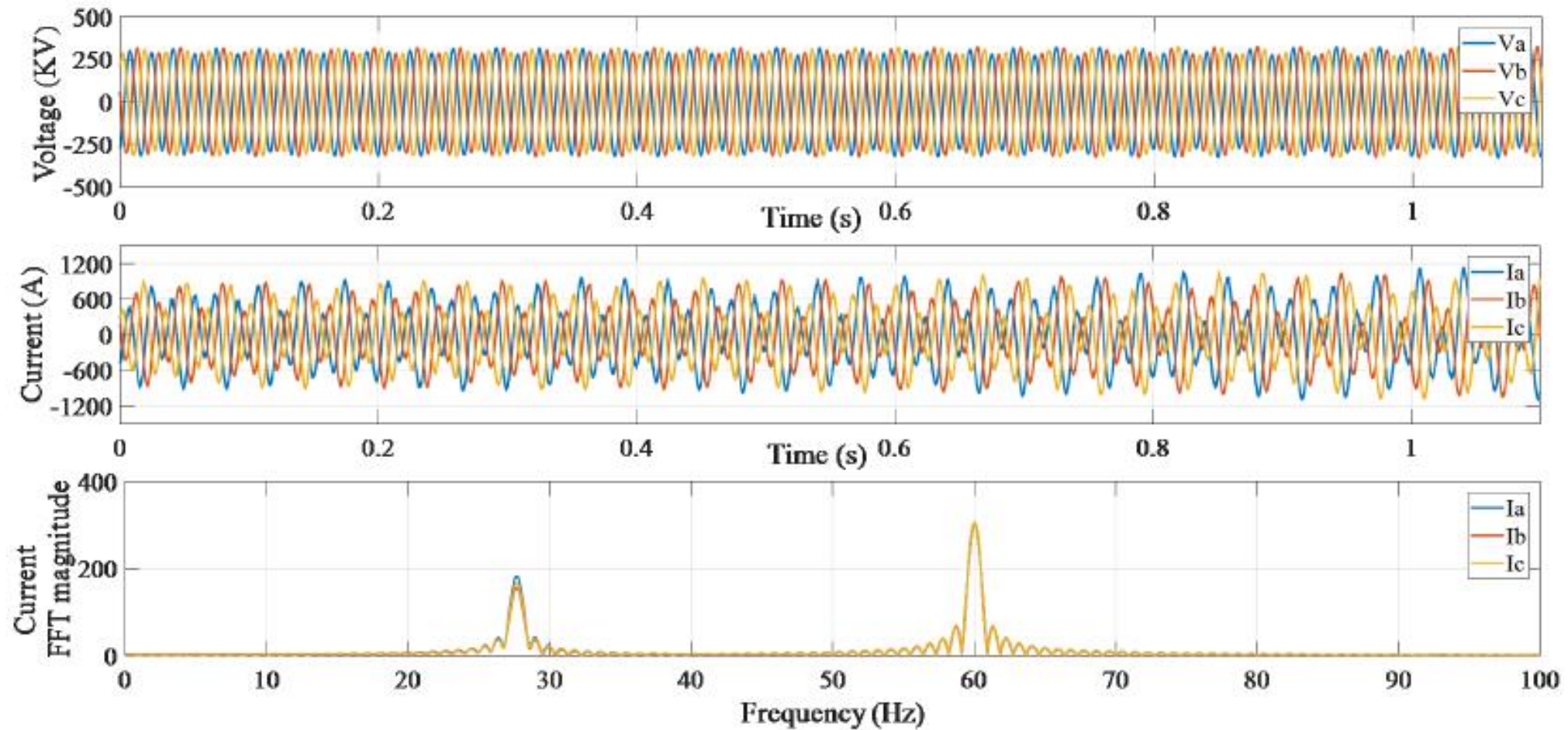


Figure 2.10: Event 1 (after Station 4 – Station 5 line section trip and before series capacitors auto-bypassed)

Reference: Chapter 2.2, Task Force Report from IEEE PES TR-80: Modeling Subsynchronous Oscillations in Wind Energy Interconnected Systems (Wind SSO TF), by Yunzhi Cheng, Jonathan Rose, John Schmall and Fred Huang

South Texas 2017 Events

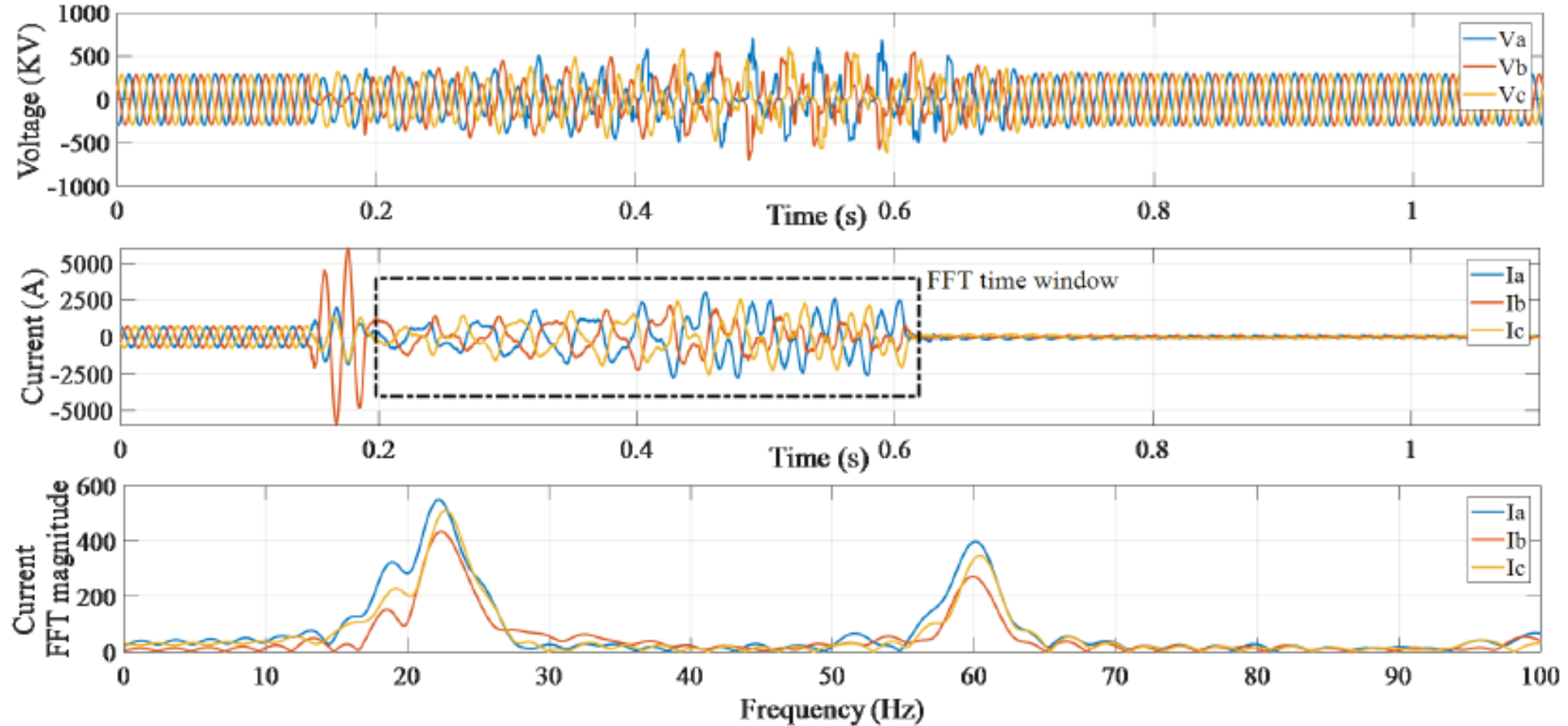


Figure 2.12: Event 2.

Reference: Chapter 2.2, Task Force Report from IEEE PES Task Force Modeling Subsynchronous Oscillations in Wind Energy Interconnected Systems (Wind SSO TF), by Yunzhi Cheng, Jonathan Rose, John Schmall and Fred Huang

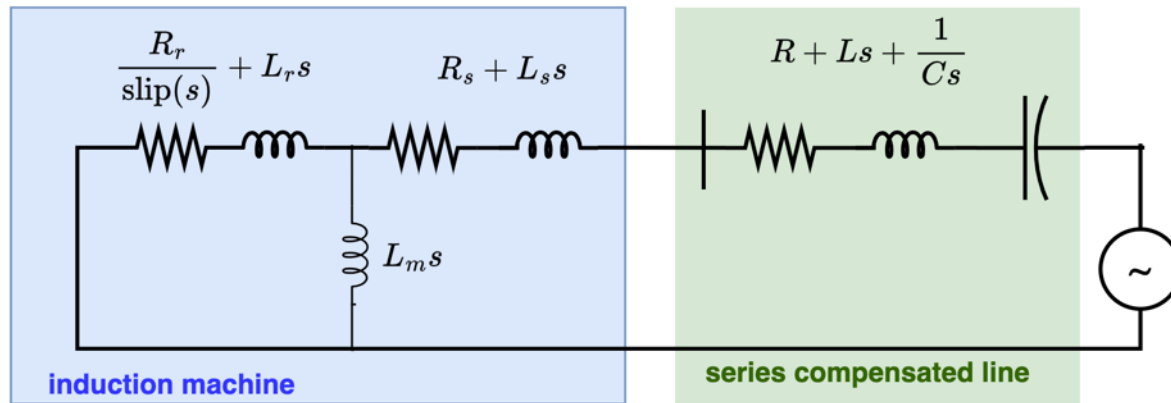
January 24 & March 10, 2023 SSO Events in AEP (Rob O'keefe)

228 MW WF interconnecting to middle of a 345 kV line series compensated at one end, WF generating near its MW capacity. The non-series compensated line section faulted and cleared in 2.5 cycles leaving **WF radial to series cap**. Sub-synchronous control interaction (SSCI) immediately apparent High peak magnitude line currents (4000+ Amp peak) High peak magnitude line voltages (600+ kV peak) Dominant sub-synchronous frequency of **21 Hz**. WF tripped in slightly less than 0.5 seconds due to high main power transformer differential current (87R)

Four WFs totaling 937 MW capacity interconnecting toward one end of a (different) 345 kV line series compensated at two locations. Two different transformer bushing faults at station at one end of line leaves **WFs radial to both series caps** and other wind/solar farms downstream. Sub-synchronous control interaction (SSCI) immediately apparent

- PSCAD model can recreate event with good fidelity
- Type 3 WFs having difficulty controlling SSCI even when detailed PSCAD SSO control tuning studies have been performed
 - – SS frequencies may change as new IBR projects interconnect nearby

SSR: induction generator effect



$$\text{slip} = 1 - \frac{\omega_m}{\omega_s} = 1 - \frac{j\omega_m}{j\omega_s} = 1 - \frac{j\omega_m}{s}$$

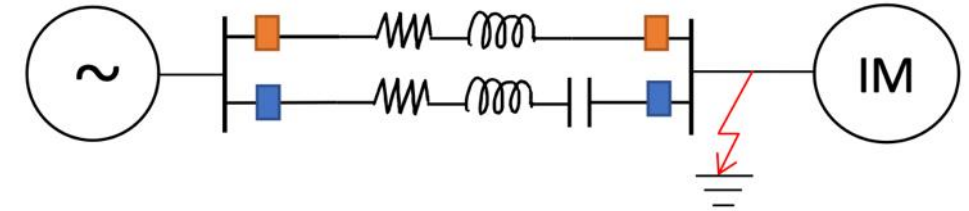
ω_s : the stator frequency or the synchronizing speed ω_m : the rotating speed

$\text{slip}(j\omega) < 0$, if $\omega < \omega_m$

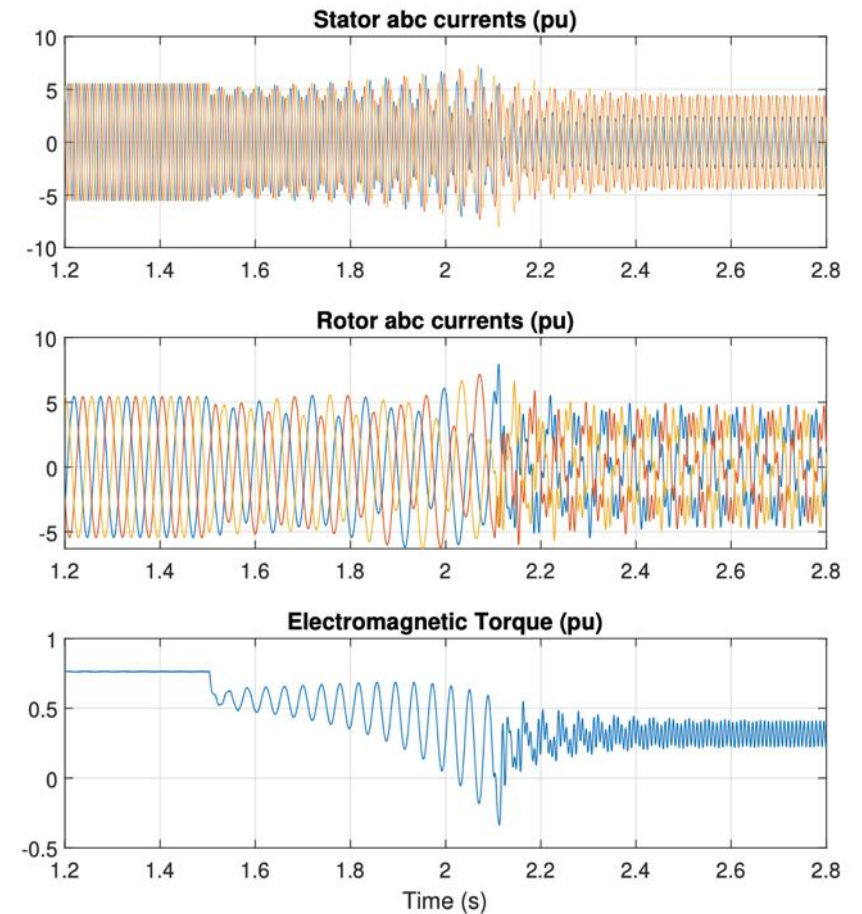
At $t = 1.5\text{s}$, the RL circuit tripped. SSR starts.

At $t = 2.1\text{s}$, a single-line-to-ground fault occurs at the IM terminal. SSRs mitigate.

Miao, Z. and Fan, L., 2022. A laplace-domain circuit model for fault and stability analysis considering unbalanced topology. *IEEE Transactions on Power Systems*, 38(2), pp.1787-1790.

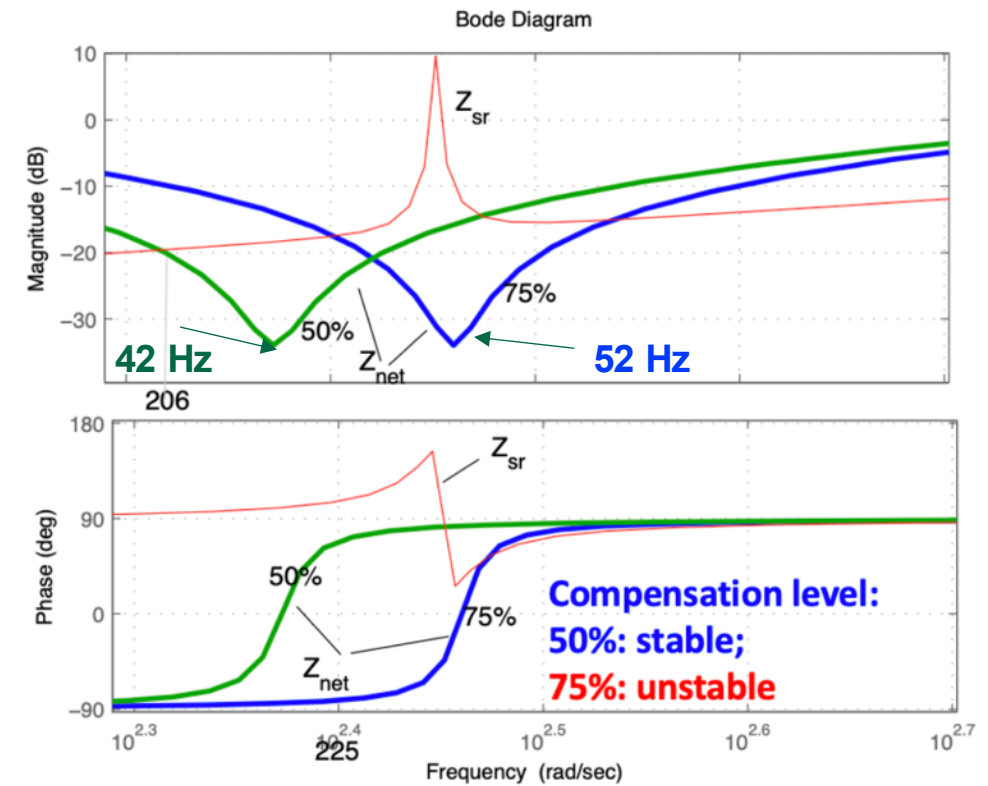
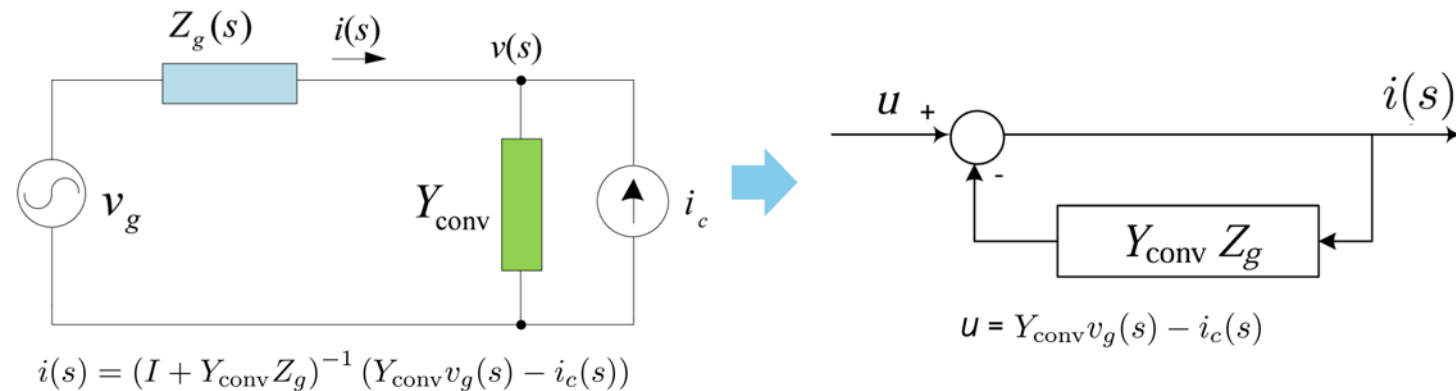


(a)



(b)

Stability analysis



Historic notes:

1. **Frequency-domain stability analysis:** Nyquist, Bode
2. Convert a **circuit analysis problem** into a **feedback system**: RD Middlebrook, J Undrill (in the 1970s)

Additional analysis: why unbalance helps SSR?

$$v_a(t) = 0, i_b(t) = i_c(t) = 0.$$

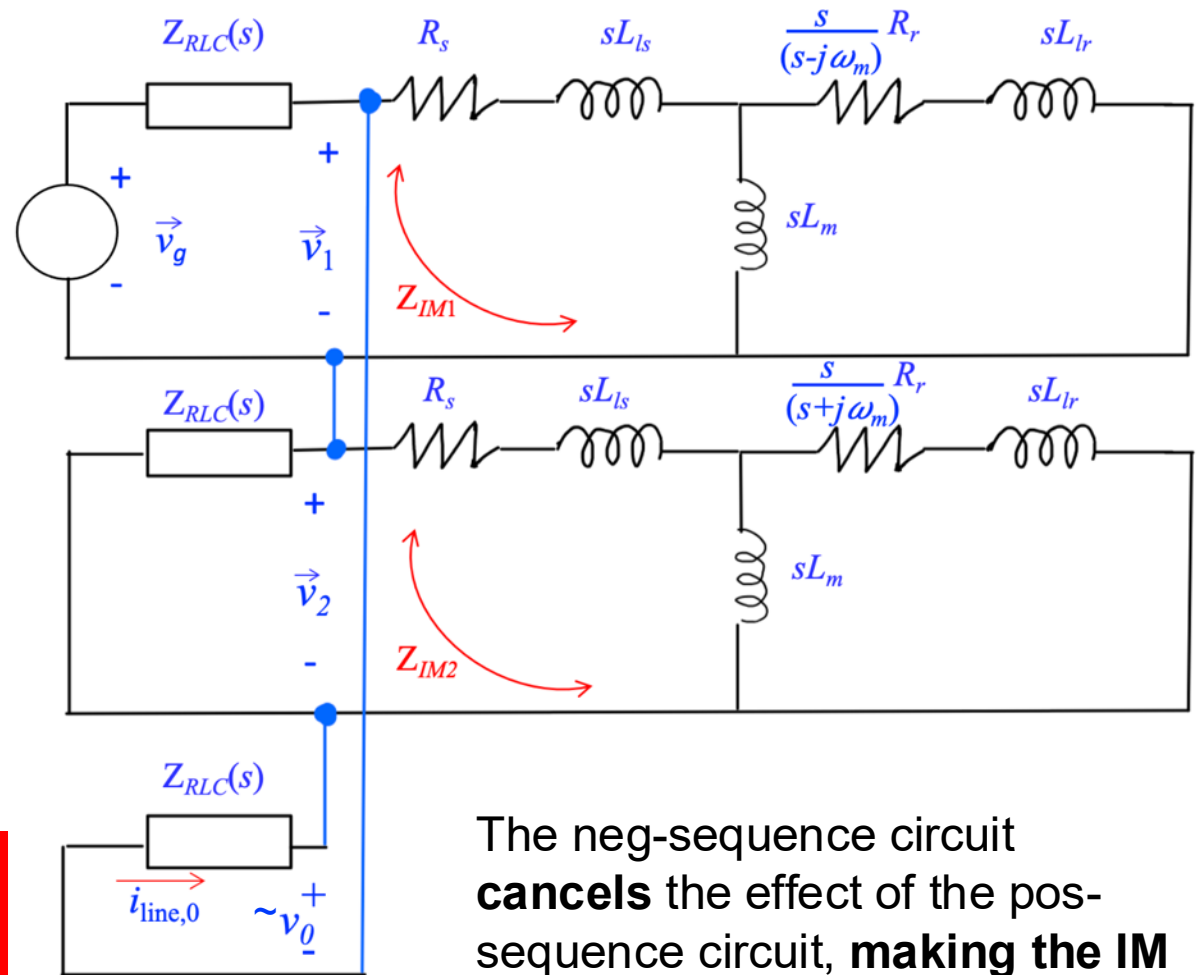
$$\begin{aligned}\frac{\vec{v}}{2} &= \frac{1}{3} \left(v_a + e^{j\frac{2\pi}{3}} v_b + e^{-j\frac{2\pi}{3}} v_c \right), \\ \frac{(\vec{v})^*}{2} &= \frac{1}{3} \left(v_a + e^{-j\frac{2\pi}{3}} v_b + e^{j\frac{2\pi}{3}} v_c \right), \\ v^0 &= \frac{1}{3} (v_a + v_b + v_c).\end{aligned}$$

$$v_a = 0, \implies \frac{\vec{v}}{2} + \frac{(\vec{v})^*}{2} + v^0 = 0,$$

$$i_b = i_c = 0, \implies \frac{\vec{i}}{2} = \frac{(\vec{i})^*}{2} = i^0 = \frac{1}{3} i_a.$$

$$\vec{v}(t) = \vec{v}_1(t) + [\vec{v}_2(t)]^*$$

$$\begin{aligned}\vec{v}_1 + \vec{v}_2 + \tilde{v}_0 &= 0. \\ \vec{i}_1 = \vec{i}_2 = \tilde{i}_0\end{aligned}$$

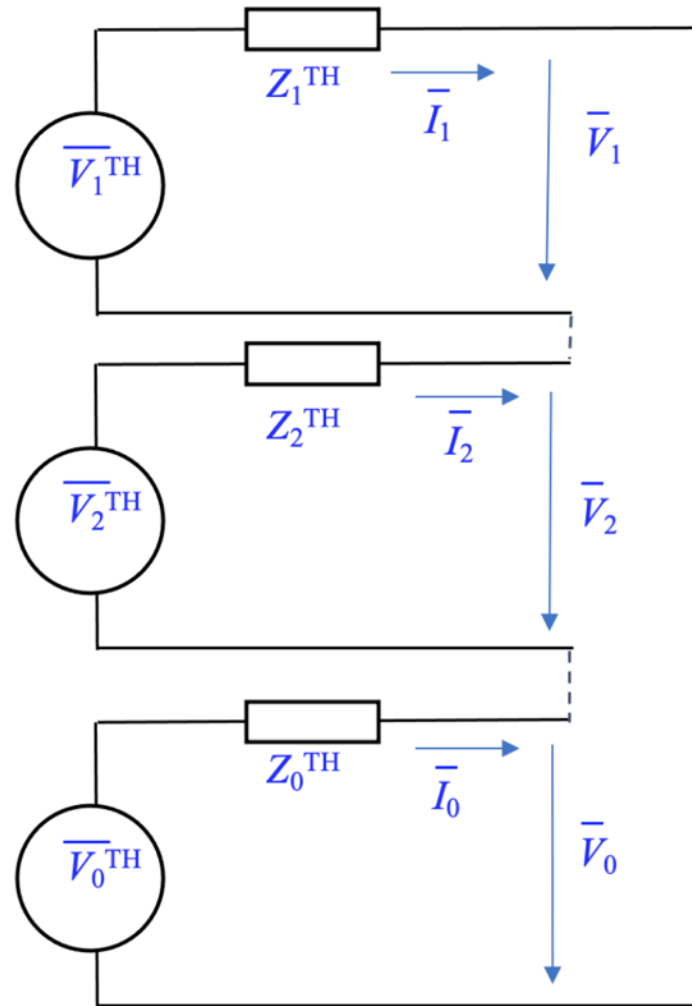
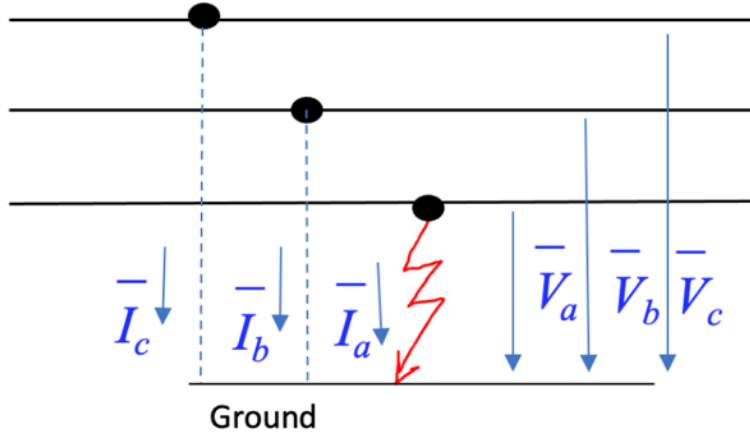


The neg-sequence circuit **cancels** the effect of the pos-sequence circuit, **making the IM passive again.**

Interconnected sequence network for quasi steady-state analysis

$$\bar{V}_a = 0, \bar{I}_b = \bar{I}_c = 0.$$

$$\bar{V}^+ + \bar{V}^- + \bar{V}^0 = 0, \bar{I}^+ = \bar{I}^- = \bar{I}^0 = \frac{\bar{I}_a}{3}.$$



Edith Clarke

Numerical analysis

For the balanced system, the loop gain is

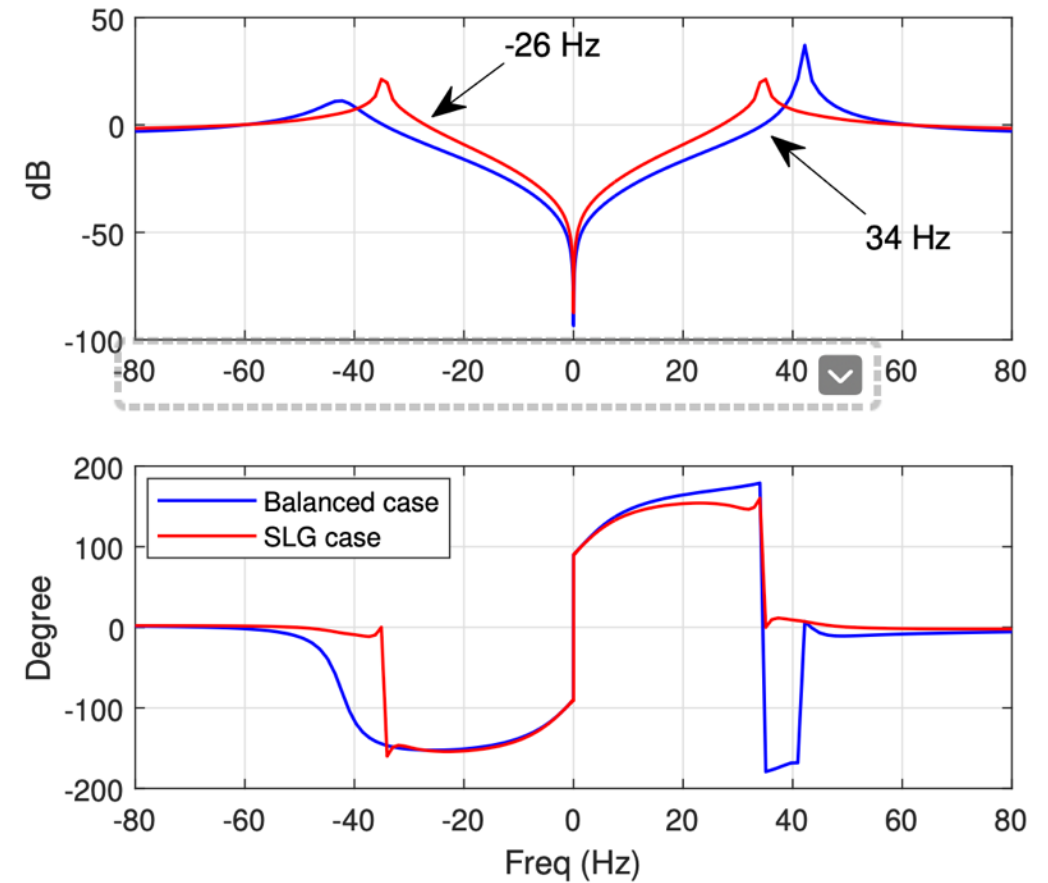
$$L_1(s) = \frac{Z_{IM1}(s)}{Z_{RLC}(s)} = \frac{R_s + \frac{s}{s-j\omega_m}R_r + s(L_{ls} + L_{lr})}{R + sL + \frac{1}{sC}}$$

For the SLG case, the loop gain is

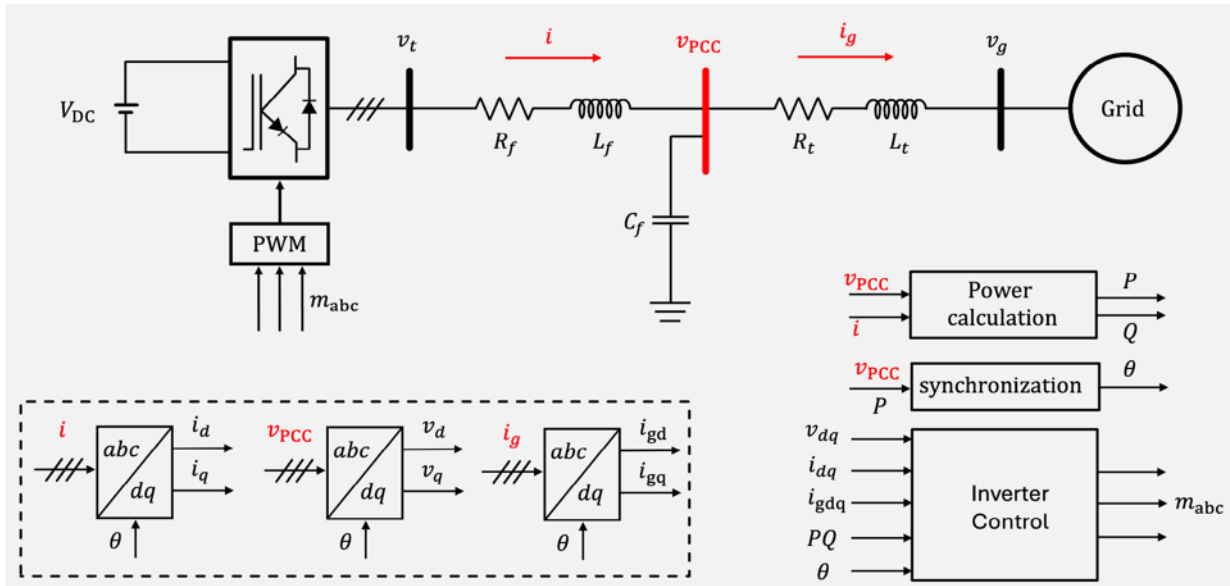
$$L_2(s) = \frac{Z_1(s) + Z_2(s)}{Z_{RLC}(s)},$$

where $Z_1(s)$ and $Z_2(s)$ are

$$Z_1(s) = \frac{Z_{IM1}Z_{RLC}}{Z_{IM1} + Z_{RLC}}, \quad Z_2(s) = \frac{Z_{IM2}Z_{RLC}}{Z_{IM2} + Z_{RLC}}.$$



Application 2: Make an inverter as a positive-sequence current source



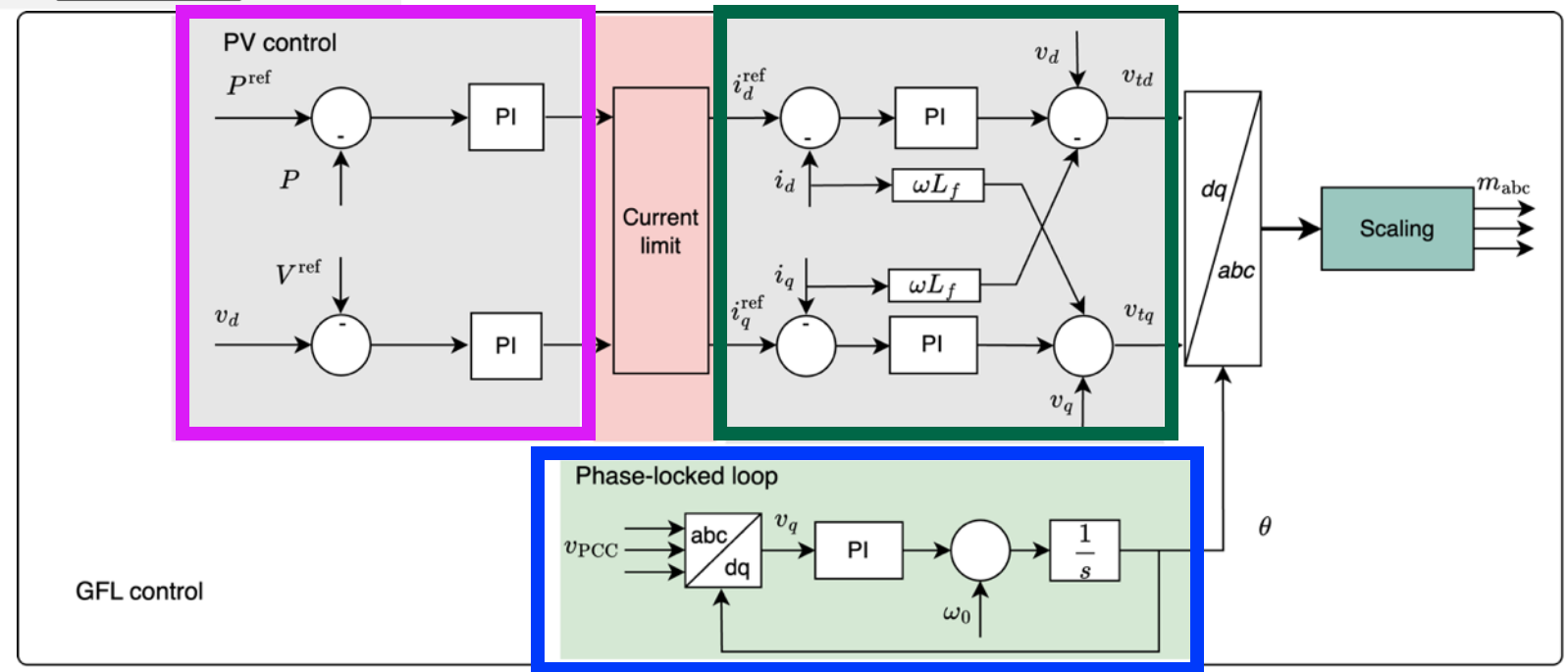
Dq-frame control:

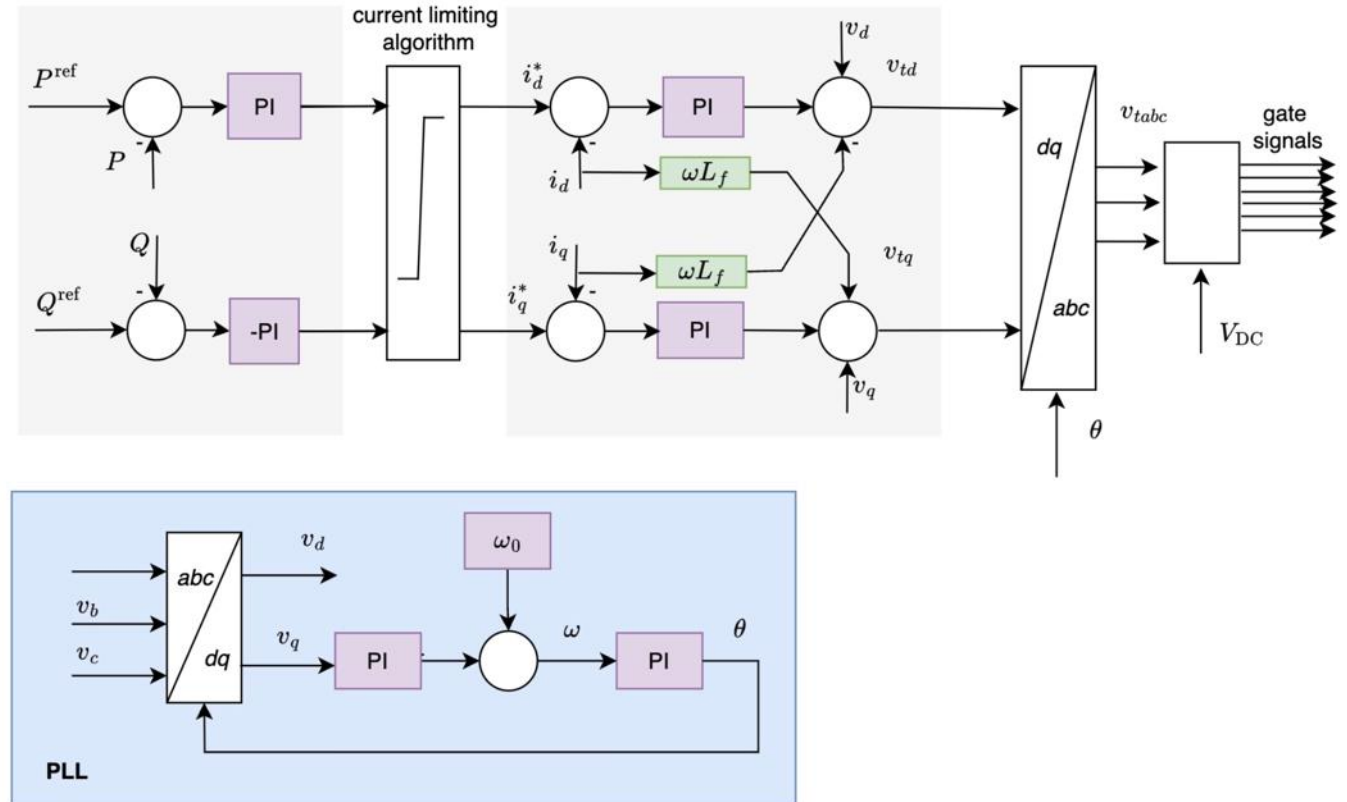
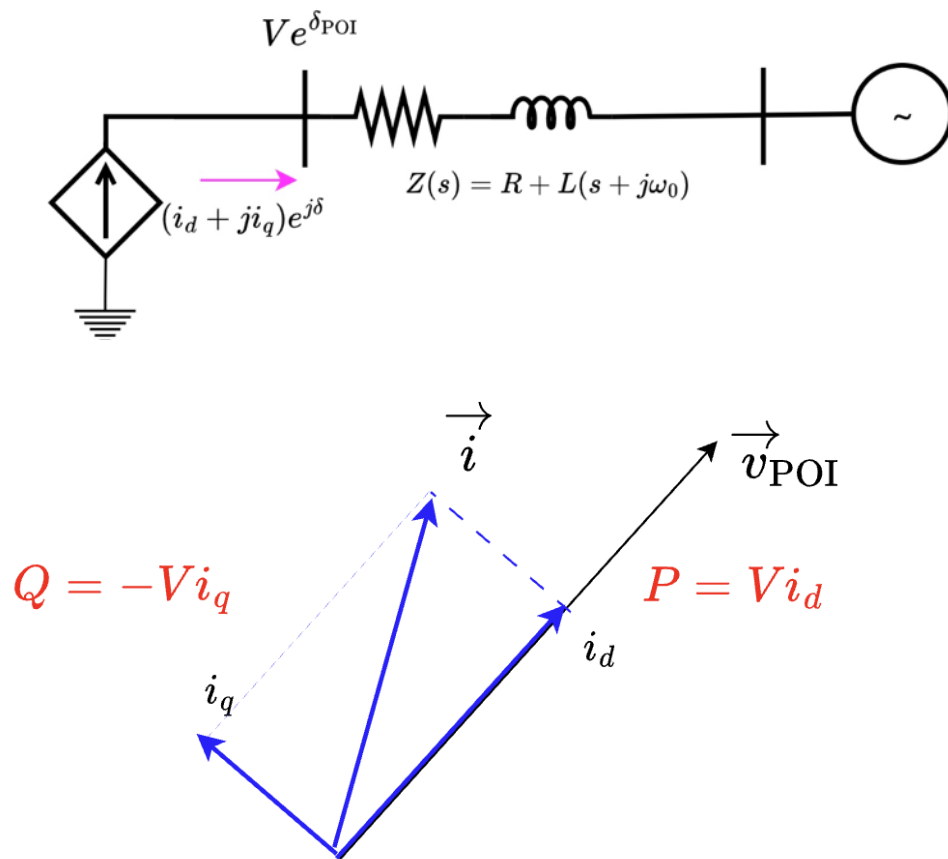
The frame aligns with the point of common coupling (PCC) voltage space vector at steady state.

Voltage-based synchronization:
PLL

Inner current control

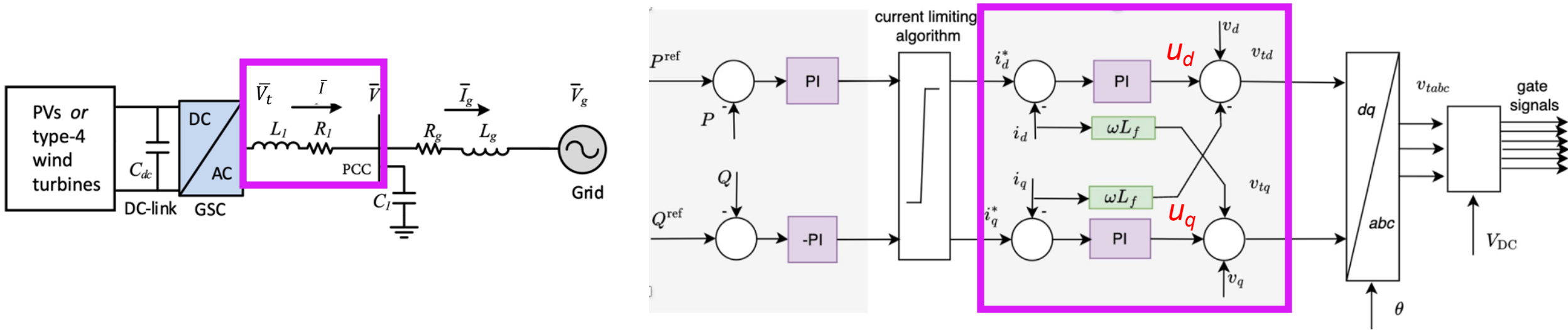
Outer power control





Decoupled vector control adapted from field-oriented control for AC motors (1968):
Technische Universität Darmstadt's K. Hasse and Siemens' F. Blaschke

The design is based on the **positive-sequence current** space vector.



In converter control design, the inner current control has the **PCC bus voltage feedforward unit**, ensuring that the converter is transformed into a **current source (bandwidth > 150 Hz, sub-cycle time scale)**.

$$\vec{v}_t - \vec{v} = (R + Ls) \vec{i}$$

$$v_{td} + jv_{tq} - (v_d + jv_q) = (R + L(s + j\omega))(i_d + ji_q); \quad \text{Viewed in the PLL frame}$$

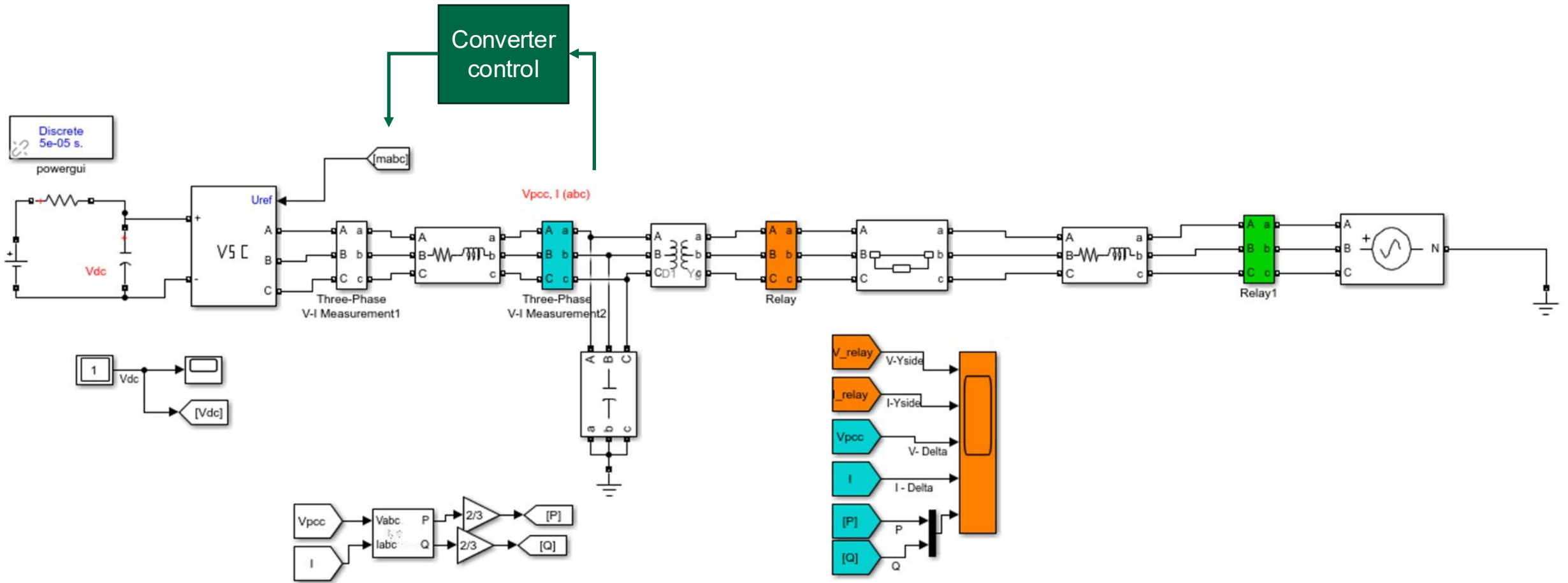
$$\underbrace{\left(K_p + \frac{K_i}{s}\right)}_{G_{PI}} (\bar{I}^* - \bar{I}) = \bar{u} = (R + Ls) \bar{I}.$$

$$\frac{\Delta \bar{I}}{\Delta \bar{I}^*} = \frac{G_{PI}}{G_{PI} + R + Ls} = \frac{K_p s + K_i}{Ls^2 + K_p s + K_i}$$

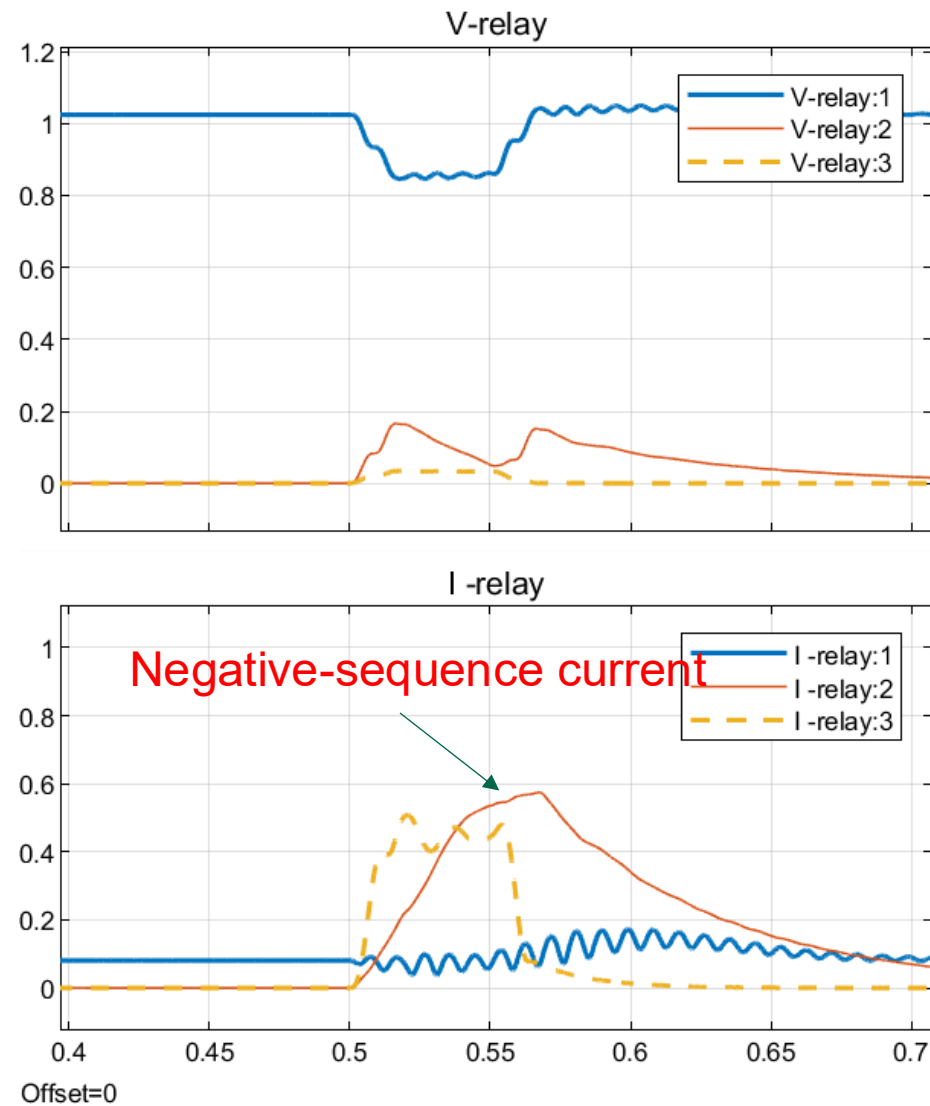
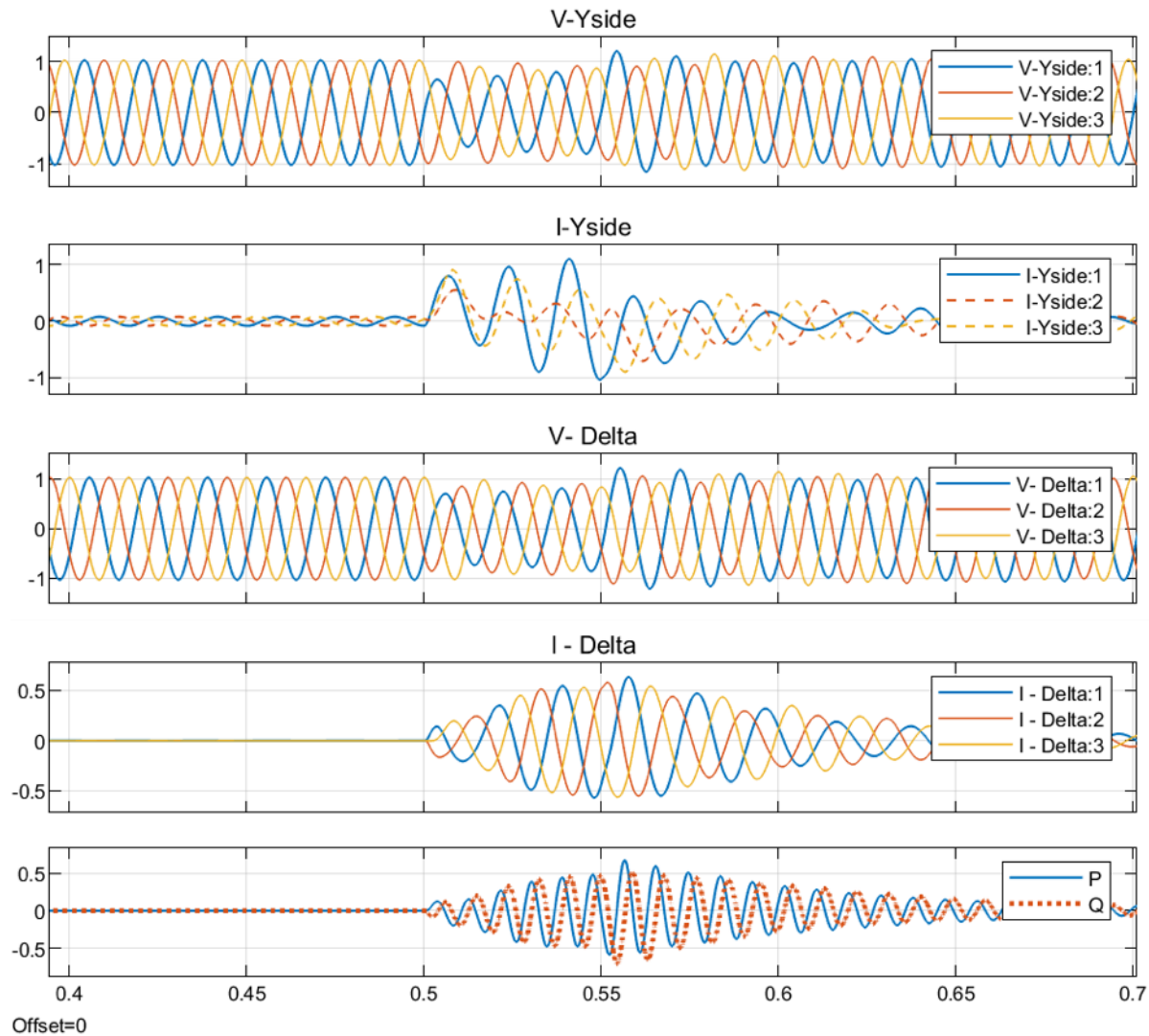
Ideally: a current source

Due to effect of the filters in the feedforward units, **there are negative-sequence currents generated.**

Electromagnetic transient simulation



No neg-sequence control



Regulate the negative-sequence current to 0

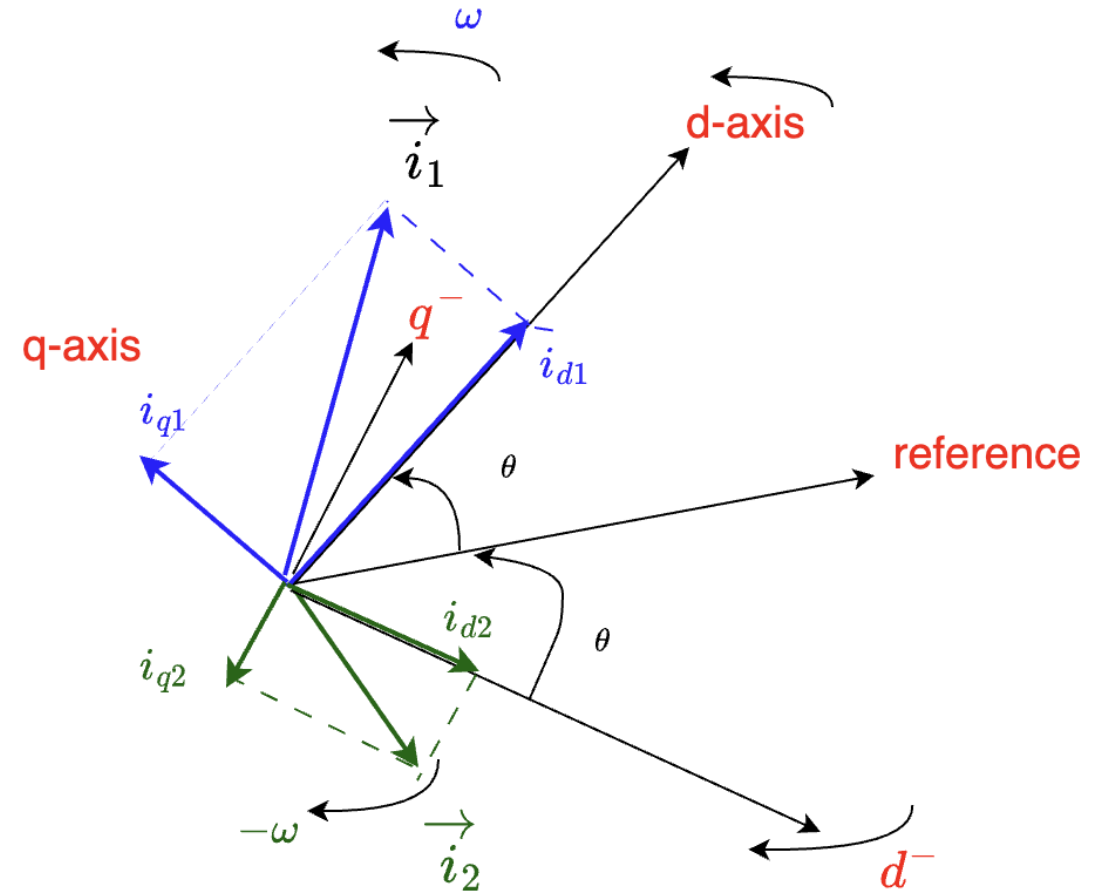
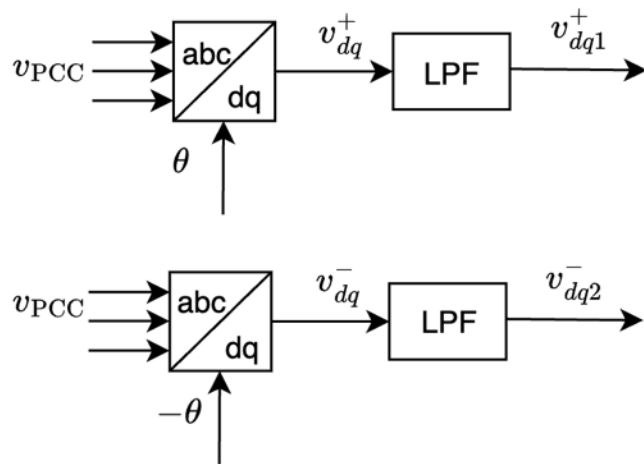
$$\vec{v}_t - \vec{v} = (R + Ls)\vec{i}$$

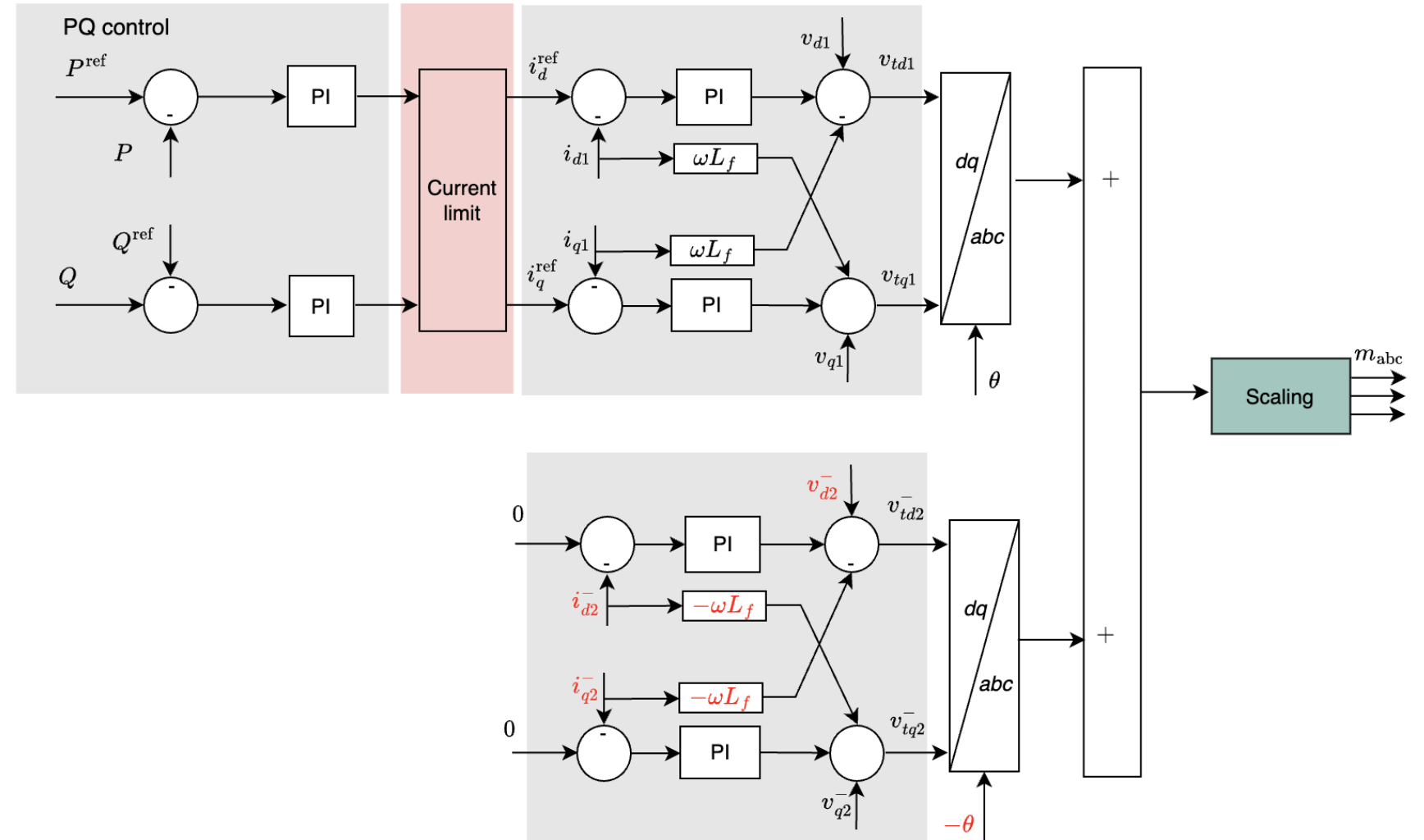
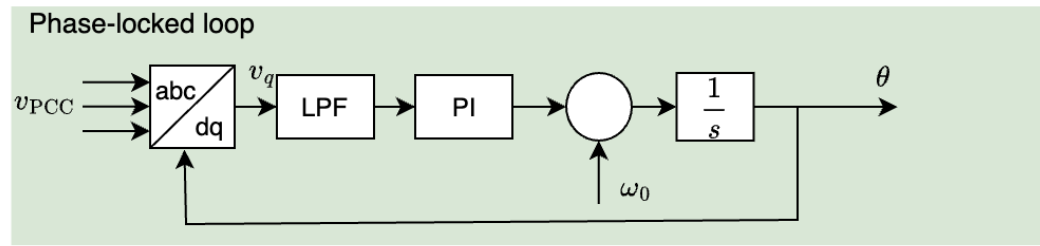
$$(v_{td2} + jv_{tq2})e^{-j\omega t} - (v_{d2} + jv_{q2})e^{-j\omega t} = (R + Ls)(i_{d2} + ji_{q2})e^{-j\omega t}$$

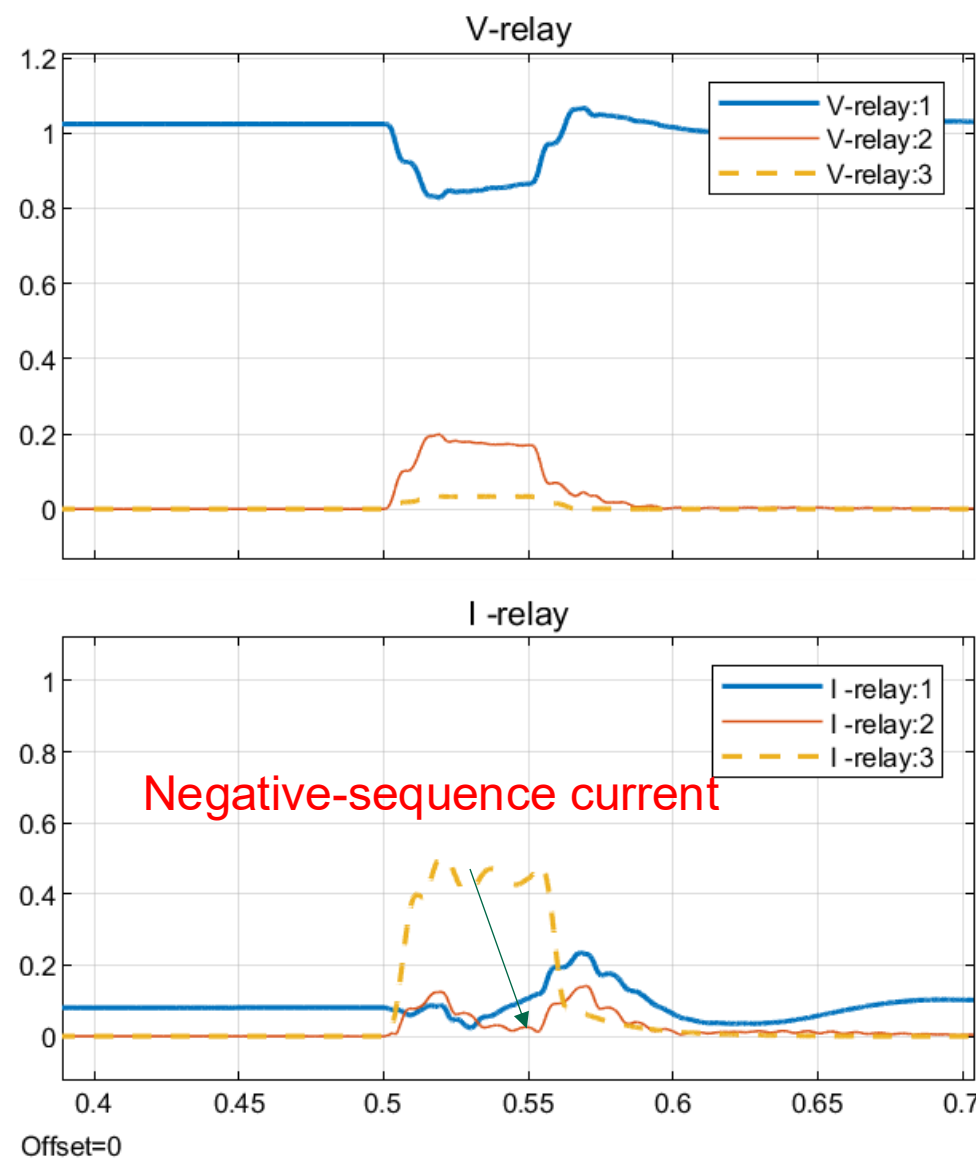
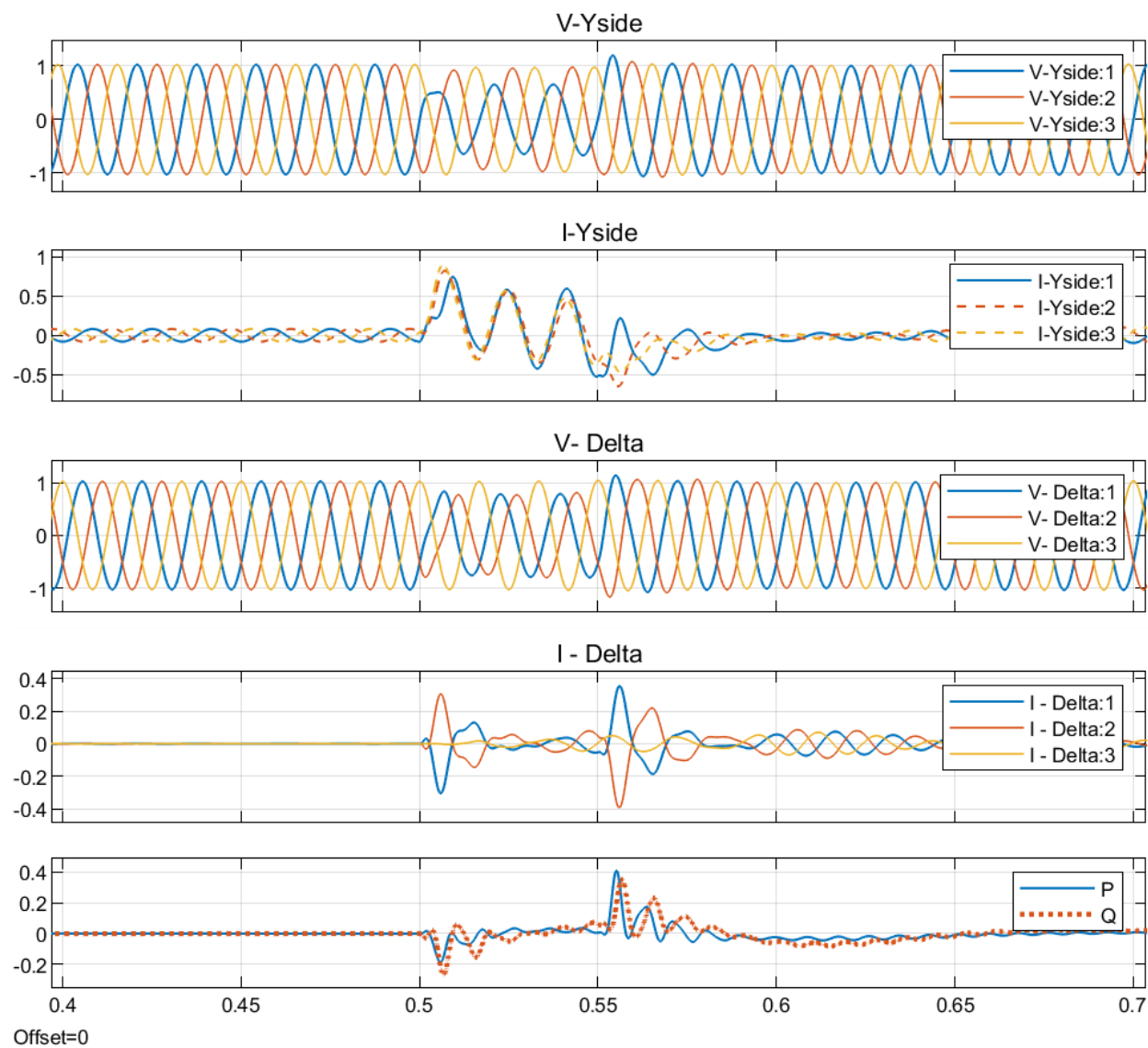
$$(v_{td2} + jv_{tq2}) - (v_{d2} + jv_{q2}) = (R + L(s - j\omega))(i_{d2} + ji_{q2})$$

$$(R + Ls)i_{d2} = \underbrace{v_{td2} - v_{d2} - \omega Li_{q2}}_{u_d}$$

$$(R + Ls)i_{q2} = \underbrace{v_{tq2} - v_{q2} + \omega Li_{d2}}_{u_q}$$

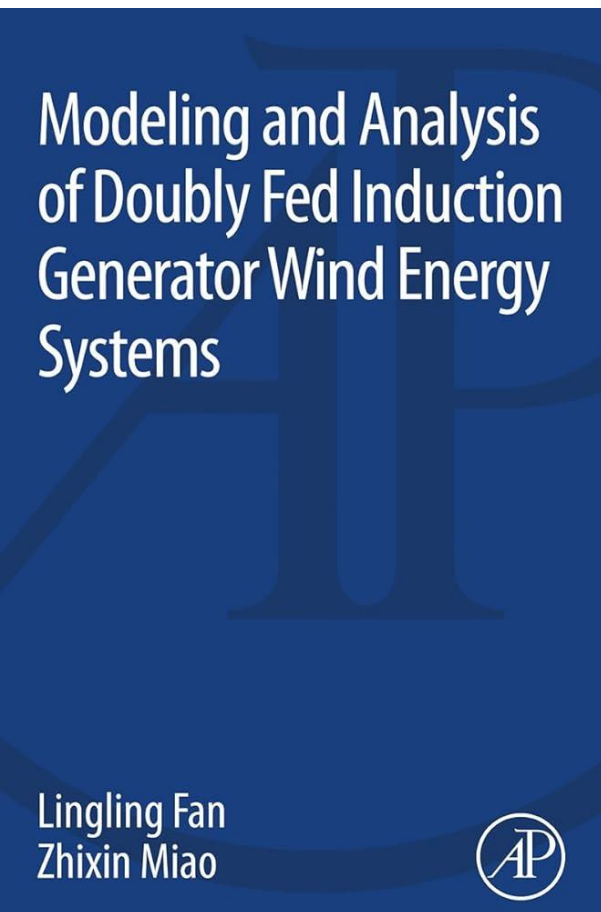




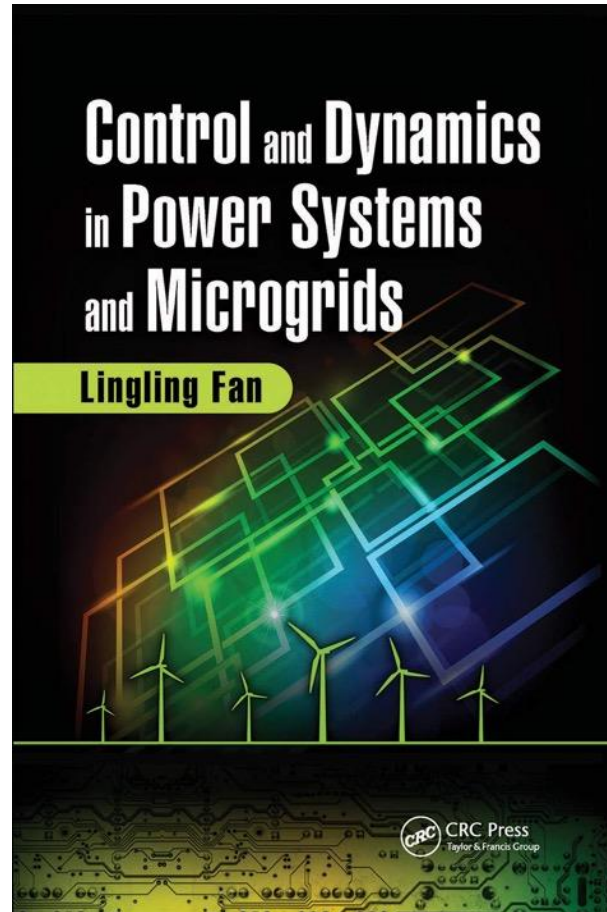


Concluding Remarks

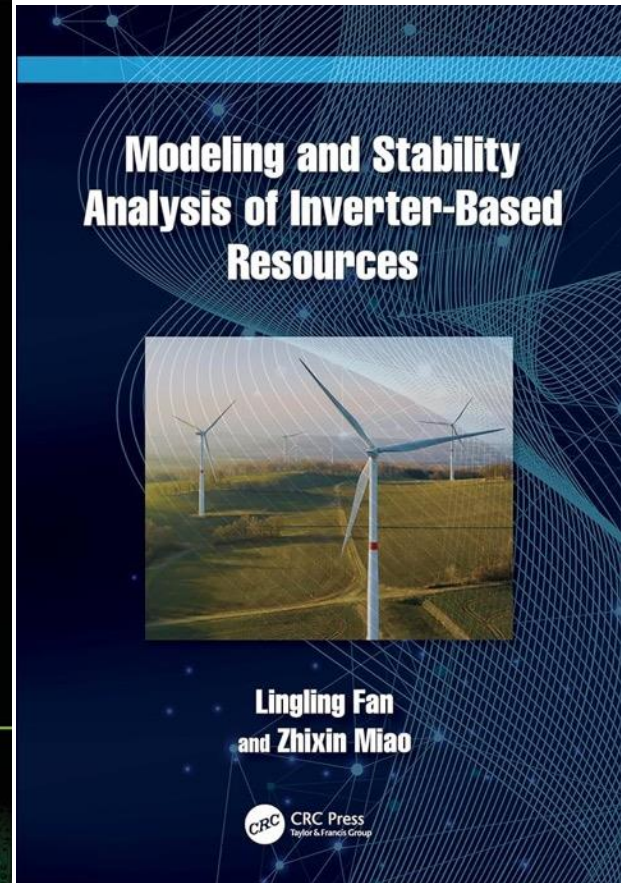
- **Control theory is very useful.**
 - Nyquist, Bode.
- Implementing it for real-world problem-solving requires integrating it with **domain knowledge**.
 - **Space vector & frame conversion**
 - **Convert circuit analysis problems into feedback systems**
- Tools in **IBR-rich power system** dynamical studies:
 - Validation tool: electromagnetic transient (**EMT**) simulation
- Resources to come up with problems
 - Industry: NERC, ESIG, CIGRE, ERCOT



2015



2017



2023

**WEAK GRID INTEGRATION OF
INVERTER-BASED RESOURCES**
Challenges and Control Solutions

Zhixin Miao
University of South Florida
Lingling Fan
University of South Florida

LOGO

To be published, IEEE Wiley